UNDERSTANDING THE TERRESTRIAL DISTRIBUTION OF STREAM-BREEDING SALAMANDERS

by

SHELBY M. BAUER

(Under the Direction of Seth J. Wenger and John C. Maerz)

ABSTRACT

The abundance and terrestrial habitat use of stream-breeding salamanders are closely linked to moisture gradients in the air and soil, which in turn are shaped by local hydroclimate and hillslope hydrology. In this study we used hierarchical modeling in a Bayesian framework to integrate multiple salamander abundance datasets to estimate how moisture gradients affect spatial patterns in the terrestrial abundance of stream-breeding plethodontids. Consistent with our hypotheses, we found that salamander abundance decreased with distance from stream, increased with elevation, and was lower on south-facing slopes than north-facing slopes. Furthermore, we found an interaction between elevation and stream distance, such that salamanders were found in higher abundances further from streams at higher elevations. Our results have implications for stream ecosystem processes and regional stream zone management.

INDEX WORDS: stream-breeding, salamander, plethodontid, abundance, distribution, stream, moisture gradient

UNDERSTANDING THE TERRESTRIAL DISTRIBUTION OF STREAM-BREEDING SALAMANDERS

by

SHELBY M. BAUER

B.S., Oregon State University, 2015

A Thesis Submitted to the Graduate Faculty of The University of Georgia in Partial Fulfillment of the Requirements for the Degree

MASTER OF SCIENCE

ATHENS, GEORGIA

2024

UNDERSTANDING THE TERRESTRIAL DISTRIBUTION OF STREAM-BREEDING SALAMANDERS

by

SHELBY M. BAUER

Major Professors: Seth J. Wenger and

John C. Maerz

Committee: Seth J. Wenger, John C. Maerz,

Rhett C. Jackson, Katherine M. O'Donnell

Electronic Version Approved:

Ron Walcott
Dean of Graduate School
The University of Georgie
August 2024

TABLE OF CONTENTS

CHAPTER 1

INTRODUCTION

Ephemeral, seasonal, and perennial streams are linked to terrestrial ecosystems by the flow of matter and the movement of organisms (Baxter et al., 2005; Polis et al., 1997; Subalusky & Post, 2019). Transport across the terrestrial-aquatic interface can alter recipient ecosystems (Leroux & Loreau, 2008; Marcarelli et al., 2011; Vanni, 2002). This interface is spatiotemporally dynamic and shaped by the same hydrologic processes that generate flow across it (Scaife et al., 2021). Given this duality, the spatial and temporal configuration of the terrestrial-aquatic interface may indirectly affect the magnitude and distribution of transport between ecosystems.

Hillslope hydrologic connectivity and soil moisture gradients can be used to describe the spatial and temporal extent of the terrestrial-aquatic interface. In humid environments, the water table connects to seasonal and perennial streams, and often saturates near-stream soils, creating a gradient of moisture extending from streams to terrestrial uplands. These saturated areas expand in wet periods and contract in dry periods as described by the variable source area concept (Hewlett & Hibbert, 1967; Dunne et al., 1975). The terrestrial extent of these saturated areas responds to precipitation gradients, such as those that frequently occur with elevational differences. As elevation and precipitation increase, saturated areas near streams expand and soil moisture gradients relax, providing increased connectivity between terrestrial and aquatic ecosystems.

Orographic and topographic patterns in precipitation and temperature predictably shape hillslope hydrology and hydroclimate across southern Appalachia (Hwang et al., 2012, 2020) making this mountain range an ideal place to study hillslope hydrologic connectivity and soil moisture

gradients. Lower temperatures and increased precipitation at high elevations (Konrad Ii, 1996) decrease evaporative water loss. Under these humid conditions precipitation readily saturates highly infiltrative soils (Helvey et al., 1972), connecting terrestrial water tables to streams and relaxing soil moisture gradients (Hwang et al., 2012). Aspect, as an indirect measure of solar radiation, further dampens or magnifies these patterns (Hwang et al., 2012). Increased solar radiation on more southern-facing hillslopes increases evaporative water loss, and constricts soil moisture gradients, while decreased solar radiation on more northern-facing hillslopes decreases temperatures and evaporative water loss, relaxing soil moisture gradients.

Stream-breeding plethodontid salamanders are a particularly useful study system through which to explore how the configuration of the terrestrial-aquatic interface may affect transport between ecosystems. This guild of salamanders begins life as larvae in freshwater streams but forages terrestrially as adults. In doing so, they move energy and nutrients from terrestrial to aquatic ecosystems when females deposit eggs in streams and from aquatic to terrestrial ecosystems following metamorphosis when juveniles join adults in terrestrial habitats. In terrestrial environments, these salamanders are sensitive to water availability and evaporative water loss (Feder, 1983). Therefore, the abundance and terrestrial habitat use of plethodontid salamanders is closely linked to moisture gradients in the air and soil (Camp, 2024).

Studies have shown that the terrestrial abundance of stream-breeding plethodontids increases with elevation, presumably due to increasing precipitation and cooler temperatures reducing evaporative water loss (Ford et al., 2002; Hocking et al., 2021). Salamander abundance also decreases with increasing distance from a stream, presumably due to decreasing soil moisture and increasing costs of dispersal (Connette et al., 2016; Crawford & Semlitsch, 2007, 2008; Hocking et al., 2021). Researchers have noted that stream-breeding salamanders may range

further from streams at higher elevation (Connette et al., 2016; Ford et al., 2002; Hairston, 1987; Petranka & Smith, 2005) and the abundance of plethodontids can be greater on cooler, wetter northern-facing aspects (Semlitsch et al., 2014). However, no study has explicitly examined the combination of these spatial patterns on stream salamander abundance and distributions.

Here we used hierarchical modeling in a Bayesian framework to integrate multiple salamander abundance datasets with different sampling designs to estimate how moisture gradients affect spatial patterns in the terrestrial abundance of stream breeding plethodontids. Our objective was to estimate the abundance of these salamanders in relation to (i) elevation, (ii) distance to the nearest stream, and (iii) aspect. We expected that patterns of stream-breeding plethodontid abundance will mirror our knowledge of regional hydrologic connectivity and soil moisture gradients, such that for a given distance from a stream their abundance will increase with elevation (Figure 1.1). We expect this pattern to be more pronounced on more northern-facing hillslopes than on southern-facing hillslopes (Figure 1.1).

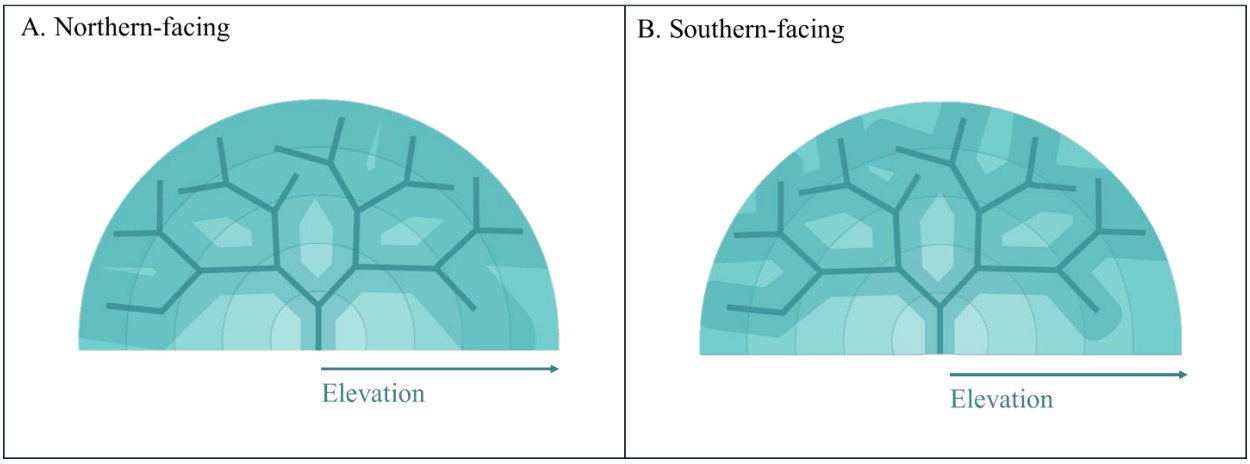

Figure 1.1. Expected stream-breeding salamander terrestrial habitat use across an elevational gradient in a northern-facing watershed and a southern-facing watershed.

CHAPTER 2

METHODS

2.1 Datasets

We integrated count and covariate data from four projects, including data collected for the purposes of this study (Table 2.1). From 2016 to 2019, data were collected using a Robust Design (Pollock, 1982) among 72 25 m^2 plots distributed across rainfall, hillslope position, and aspect gradients [hereafter "gradient study"] (Howard, 2018). From 2018-2020 we sampled an additional 18 plots within two watersheds used for the U.S. Forest Service's "Future Forest Experiment" [hereafter FFE] using the same robust design (Head, 2020). Both studies were based within the Coweeta Basin of the Coweeta Hydrological Laboratory, a US Forest Service Research Station and former National Science Foundation Long-Term Ecological Research site in Macon County, North Carolina (Figure 2.1). In 2021, we modified our sampling design to use a depletion sampling approach. This design was used to sample the FFE plots in 2021, 2022, and 2023, and the gradient plots in 2022. In 2021 we also began collecting data, using the depletion design, at 339 plots among 24 sites spanning north Georgia, western North Carolina, and eastern Tennessee for a "Hemlock" management study. For this study, we added an additional 65 plots in the Coweeta basin, 20 plots in the adjacent Dryman Fork watershed that is also part of the Coweeta Hydrologic Laboratory, and 6 plots on Grandfather Mountain in Avery County, North Carolina.

In total, our integrated datasets encompass 511 25m^2 plots among 73 sites across the southern Blue Ridge Mountains within the Chattahoochee, Nantahala, and Pisgah National Forests and Great Smoky Mountains National Park (Figure 2.1). Our study plots ranged from 595 m to 1429

m elevation, with four sites reaching into the “High Mountains.” Forty-eight of the 73 sites were located within Coweeta Hydrologic Laboratory. The remaining 26 sites stretched across northeastern Georgia, eastern Tennessee, and western North Carolina (Figure 2.1).

2.2 Study area

The southern Blue Ridge Mountains are characterized by high-gradient, bedrock and boulder-bottomed, cool, clear streams that drain Appalachian oak forests, cove forests, and northern hardwood forests from 260 m to 1645 m and southeastern spruce-fir forests, northern hardwoods, and grass-heath balds from 1370 m to 2026 m in the High Mountains (Griffith et al., 2002). Precipitation across the region is abundant and frequent throughout the year, ranging from 1270 mm at lower elevation to over 2540 mm in the High Mountains (Griffith et al., 2002; Konrad Ii, 1996). Soils are highly infiltrative, and infiltration-excess surface runoff rarely occurs (Helvey et al., 1972).

2.3 Study species

Our datasets included data on all observed salamanders, but we focused our analyses on the Mountain Dusky complex (*Desmognathus* spp.) and the Blue-Ridge Two-Lined salamander (*Eurycea wilderae*). The Mountain Dusky species in our study included the recently differentiated *D. adatsihi* and *D. ocoee* (Pyron & Beamer, 2022b), as well as *D. orestes* (Pyron & Beamer, 2022b). Our focal species complexes represent a guild of semiaquatic Southern Appalachian plethodontids that are known to disperse well beyond the stream margins into terrestrial uplands where they forage. This guild is colloquially referred to as stream-breeding salamanders, which includes several larger, more aquatic species such as *Pseudotrition ruber*, *Gyrinophilus porphyriticus*, *D. conanti*, *D. monticola*, *D.folkertsi*, and several newly described

species formerly identified as *D. quadramaculatus* (Pyron & Beamer, 2022a) or *D. marmoratus*. These species typically do not venture far from the stream margin (Hairston, 1949; Organ, 1961). Because of their limited terrestrial movements these species are not well represented in our data and were excluded from our analyses.

We chose to model Mountain Dusky and Blue Ridge Two-Lined salamanders separately because of known differences in their habits and life history traits. In areas closer to streams, Mountain Dusky salamanders tend to be more numerous than Blue Ridge Two-Lined salamanders (Petranka & Murray, 2001), and have been found to nest in association with a broader collection of surface waters (seeps, springs, wet rock faces, and low order streams) compared to Blue Ridge Two-Lined salamanders, which mostly breed in perennial streams. (Keen & Orr, 1980; King, 1939; Tilley, 1973). The difference in surface water use is presumably due to the shorter larval periods of the Mountain Dusky Salamanders compared to the Blue Ridge Two-Lined salamander (Lannoo, 2005).

2.4 Study design

2.4.1 Count data collection

Across all four projects we collected abundance data using time and area-constrained searches and one of the two sampling designs. As mentioned previously, from 2016 through 2020 we collected data at Coweeta using a form of Pollock's Robust Design (Pollock, 1982). Under this framework, plots were sampled on three, usually consecutive, nights in the spring, summer, and fall. Surveys began at least 50 minutes after sunset once the sky was wholly dark and concluded before dawn (usually before (0200 h). During a survey, one or two observers evenly searched the entire plot area for at least 15 person-minutes. Total search time could be longer than 15 person

minutes when thick vegetation or capturing many salamanders required more time for equal search effort.

Observers did not overturn cover objects or disturb leaf litter but visually searched the ground and leaf litter surface, the surface of downed wood, tree trunks, shrubs, and herbaceous vegetation. When observed, salamanders were captured using a nitrile-gloved hand and placed into an individually labeled Ziplock bag. When a salamander was visible but inaccessible for capture or in a position that allowed for a high probability of escape, surveyors recorded as much information on the animal as possible before attempting to capture the individual.

A challenge with the approach above is that it assumes that populations are closed and that individuals are equally available for capture each night. This is problematic when studying plethodontid salamanders because there can be large fluctuations in their surface activity from one night to another in response to changes in weather, and only salamanders that are active at the surface are available for capture. To address this shortcoming, in 2021 we began collecting data across our entire study area using a depletion design. Under this framework, plots were sampled in four consecutive "passes." During a pass an observer searched the entire plot for a minimum of 3.75 minutes. Thus, each plot was searched for at least 15 minutes, making the total sampling effort on a given night equivalent to the prior sampling design. However, each plot was now sampled only during a single night in the spring, summer, and fall. An exception were the plots sampled in 2023 for the Future Forests project, which were sampled monthly, June through October, using the depletion design. This modified method allowed us to estimate the effects of weather on nightly surface activity and separate salamander availability from conditional capture probability. In addition, the more efficient design allowed us to increase the number of study plots and sites, improving our spatial representation and parameter precision (Bradke, 2023).

Under both designs, all salamanders that were captured were identified to species, measured, assigned an age class, and sexed. Observers recorded snout-vent length and total length to the nearest mm, and wet mass to the nearest 0.01 g. Snout-vent length was used to assign age class (hatchling, juvenile, sub-adult, or adult). Sex was determined by the presence of secondary sexual characteristics. Males were identified using the presence of enlarged nasal cirri, a mental gland, premaxillary teeth, visible testis, or a swollen vent. Females were identified by the absence of male traits if their snout-vent length indicated they were likely sexually mature or by the presence of developing eggs (Rucker et al., 2021).

2.4.2 Observed covariate data collection

After at least 10 minutes or after end of the 3rd pass, an observer who was not actively searching the plot recorded weather and habitat variables. Air temperature and relative humidity were recorded using a Kestrel™ 3000 Weather Meter (KestrelMeters.com). Additional qualitative measures of weather and habitat were recorded but were not utilized in our analyses. Under the depletion design, observers also recorded ground vegetation coverage below eye level and perceived visual obstruction in units of 20%. Ground vegetation coverage is thought to influence an observer's ability to detect surface-active salamanders whereas perceived visibility was intended to approximate how well an observer believed they could see surface active animals.

2.5 Data Analyses

We used an integrated hierarchical modeling approach in a Bayesian framework to generate estimates of salamander abundance with data from both designs. We selected geomorphic and weather-related model covariates that represented important correlates of soil hydrology and hydroclimate in southern Appalachia. We included elevation, stream distance, and aspect as predictors of abundance, and we included vapor pressure deficit and precipitation as predictors of salamander availability. The parameters we placed on abundance reflect temporally stable proxies of soil moisture, precipitation, and humidity that we expected to affect salamander abundance. The parameters we placed on availability reflect short-term patterns in soil moisture and humidity that are expected to affect salamander surface activity (Gade et al., 2020). We chose to include ephemeral, seasonal, and perennial streams in our definition of stream because of their role in hillslope hydrology and stream-breeding salamander life history. We used vegetation coverage as a predictor of the conditional capture probability of salamanders because we expected vegetation to increase habitat complexity and make it more difficult for observers to detect salamanders.

2.5.1 Model inputs

We analyzed the count data of our focal taxa from 3,949 of the 4,282 plot-surveys conducted across our study area from 2016 to 2023. We excluded 333 surveys from three sites at Coweeta where an experimental management treatment was applied during our study period (for the FFE project). Of the surveys we analyzed, 69% (2731) were collected using the Robust Design-- all at Coweeta-- and 31% (1218) were collected using the depletion design. Of the 1218 observations made using the depletion design, 46% (560) were made at Coweeta. This means that 83% of our integrated dataset was collected at Coweeta. Count data were subset by our two focal taxa and

the model was independently fit to each species-complex for analysis because we expected each to respond differently to covariates like stream distance.

We paired count data with geomorphic, weather, and habitat data hypothesized to affect the terrestrial abundance and observation of stream breeding salamanders. Geomorphic variables included elevation, aspect, and stream distance, which were derived from 10 m resolution digital elevation models from the National Map (apps.nationalmap.gov). We created two stream layers using the Arc Hydro Toolset and workflow in ArcGIS Pro (v3.2.2; esri.com/en-us/industries/water-resources/arc-hydro). We used 3,035 m^2 (0.75 acres) to define the minimum contributing area for a stream network including ephemeral, seasonal, and perennial streams [hereafter "ephemeral stream layer"]. We came to this threshold independently by comparing preliminary iterations of the layer to on-the-ground knowledge of study sites. However, others have also found this upslope area to accurately delineate the ephemeral extent of streams in Southern Appalachia (Connette & Semlitsch, 2013). The layer failed to capture streams at three of our highest elevation sites (located in the High Mountains). In these areas we manually extended the derived stream layer to reflect on-the-ground knowledge. We derived a second stream network including only perennial streams for post-hoc analyses [hereafter "perennial stream layer"]. For this layer we used 76,890 m^2 (19 acres; Rivenbark & Jackson, 2004) to define the minimum contributing area (Figure 2.2). For both stream layers, we used the Geodesic method in the Near tool from the Spatial Analyst Toolbox to derive distance to the nearest stream. We converted aspect to "northness", defined as 1 (due north) to – 1 (due south). See Appendix B for more information about how we derived geomorphic covariates.

Weather variables included cumulative precipitation and vapor pressure deficit. Cumulative precipitation between 1 and 5 days prior to a sampling event was derived from observed daily

precipitation from NOAA's Advanced Hydrologic Prediction Services (water.weather.gov). Vapor pressure deficit was calculated from air temperature and relative humidity values recorded during surveys. These measures were not consistently recorded during surveys in 2016, 2017, and 2018 due to limited or faulty equipment. We fit random forest models to interpolate these missing values using the Ranger package (v 0.16.0; Wright, 2013) with 500 trees to optimize split, node size and sample size. We used out-of-bag root mean square error and plots of measured vs predicted values to assess performance. See Appendix C for detailed methods on the optimization, fit, and evaluation of the random forest models.

We used ground vegetation coverage to approximate habitat complexity, which we considered a potential covariate on an observer's ability to detect a surface-active salamander. This variable was not recorded 2016-2020, but all plots sampled during this time were sampled in 2022, when ground vegetation coverage was recorded. Because we observed minimal season-to-season and year-to-year variation in vegetation cover at the plot scale, we applied the averaged values of ground vegetation coverage for each plot in 2022 to the 2016-2020 data set.

2.5.2 Model specification

We integrated multinomial and binomial mixture models to estimate the terrestrial abundance (λ), availability (ω), and conditional capture probability (ρ) of salamanders at each plot every year. We modeled the ecological process of abundance as a function of elevation ($Elev$), aspect ($Northness$), and stream distance ($Dist$) with an interaction between elevation and stream distance. We specified that the abundance intercept varied among plots and years to allow populations to be open among years.

$$\log(\lambda_i) = \beta_0 + \beta_1 Elev_i + \beta_2 Dist_i + \beta_3 Dist_i Elev_i + \beta_4 Northness_i$$

$$N_i \sim Poisson(\lambda_i)$$

We jointly modeled availability as a function of vapor pressure deficit (*VPD*) and cumulative precipitation 5 days prior to a sampling event (*Precip*). We included a site-specific random effect on availability to account for spatial autocorrelation amongst plots within sites.

$$logit(\omega_j) = \omega_0 + \omega_1 VPD_j + \omega_j Precip_j + SiteEffect_j$$

$$\Omega_j \sim Binonial(\omega_j, N_i)$$

We jointly estimated the conditional capture probability of the first quarter or first pass of a survey (ρ) as a function of observer-estimated ground vegetation cover and a random effect of plot visit but modeled this portion of the observation process separately for each data set. The detection process for count data collected using the Robust Design transforms this estimate (ρ) into an estimate of the conditional capture probability of a survey ($1 - (1 - \rho_k)^4$) before drawing counts from a binomial process. In contrast, the detection process for count data collected using the depletion design passes this estimate (ρ) through a multinomial process which estimates the probability a surface-active salamander is captured in the first, second, third, and fourth pass before estimating the probability that a surface-active salamander is not captured ($(1 - \rho_k)^4$).

From this multinomial process an estimate of the conditional capture probability of a survey ($1 - (1 - \rho_k)^4$) is derived and used to draw counts from a binomial process. These expected counts are then combined with the five pass-level conditional capture probabilities to draw counts from a multinomial process.

Robust Observation Process	**Depletion observation process**
$logit(\rho_k) = \alpha_0 + \alpha_1 Veg_k + VisitEffect_k$	$logit(\rho_k) = \alpha_0 + \alpha_1 Veg_k + VisitEffect_k$
$\rho.eff_k = 1 - (1 - \rho_k)^4$	$\pi_{k,1} = \rho_k$ $\pi_{k,2} = (1 - \rho_k) \times \rho_k$ $\pi_{k,3} = (1 - \rho_k)^2 \times \rho_k$ $\pi_{k,4} = (1 - \rho_k)^3 \times \rho_k$ $\pi_{k,5} = (1 - \rho_k)^4$
$y.r_k \sim Binomial(p.eff_k, \Omega_j)$	$n_k \sim Binomial((1 - \pi_{k,5}), \Omega_j)$
	$\{(y.d_{k,1:4}\} \sim Multinomial(n_k, (\pi_{k,1:4}/(1 - \pi_{k,5})))$

2.5.3 Model fit and evaluation

We fit our model using Markov chain Monte Carlo (MCMC) sampling in JAGS (Plummer, 2003) called via the jagsUI package (Kellner & Meredith, 2024) in R (4.3.3). We used three MCMC chains with 500,000 iterations, including a 300,000-iteration burn-in. We standardized all continuous covariates prior to analysis. We assessed chain convergence visually using trace plots and empirically using the Gelman-Rubin statistic ($\hat{R} < 1.1$; Gelman & Rubin, 1992).

We assessed model fit using Bayesian p-values and scatterplots of associated discrepancy measures (Gelman et al. 2021.; Schaub and Kéry 2022) as well as chi-squared p-values. We used

mean absolute error to measure the discrepancy between observed and expected survey level counts (drawn from binomial distributions), and we used the median chi-squared p-value to measure the discrepancy between observed and expected pass level counts (drawn from a multinomial distribution). The discrepancy values we used to calculate our Bayesian p-values allowed us to assess how well our model's error structure approximates or "fits" the error structure of our data. Bayesian p-values close to 0.5 indicate an appropriate error structure, whereas values more extreme than .05 or .95 can be indicative of poor fit. The median chi-squared p-value we used to assess our model's fit to pass-level counts allowed us to assess how likely our expected counts (samples drawn from all three MCMC chain) are to match the counts we observed. A chi-squared p-value greater than 0.05 indicates that we cannot reject the null, which states that our expected counts match our observed counts. To validate the model's predictive accuracy and estimate prediction error, we withheld data collected in 2023 at three sites in watershed 32 at Coweeta Hydrological Laboratory and used the fitted model to predict counts observed at the sites in 2023. The three sites selected are the only sites in our integrated dataset that were sampled every year from 2016 to 2023. They are located centrally within the elevational and latitudinal range of our data but share a southeastern aspect. Collectively they represent a relatively average area with high temporal replication.

Table 2.1 Sample design, years sampled, and number of plots associated with each component dataset in our integrated dataset.

Dataset	Sample design	Plots	Years sampled	Authors
Gradient	Robust	72	2016 -2019	(Head, 2020; Howard, 2018; Mcentire, 2018)
Future Forests	Robust, depletion	18 (2018-2022), 24 (2023- present)	2018-2019 (Robust), 2020-present (depletion)	(Head 2020; Grab 2024)
Hemlock	depletion	330	2021-2022	Maerz et al. *in prep*
Current study	depletion	85	2022	

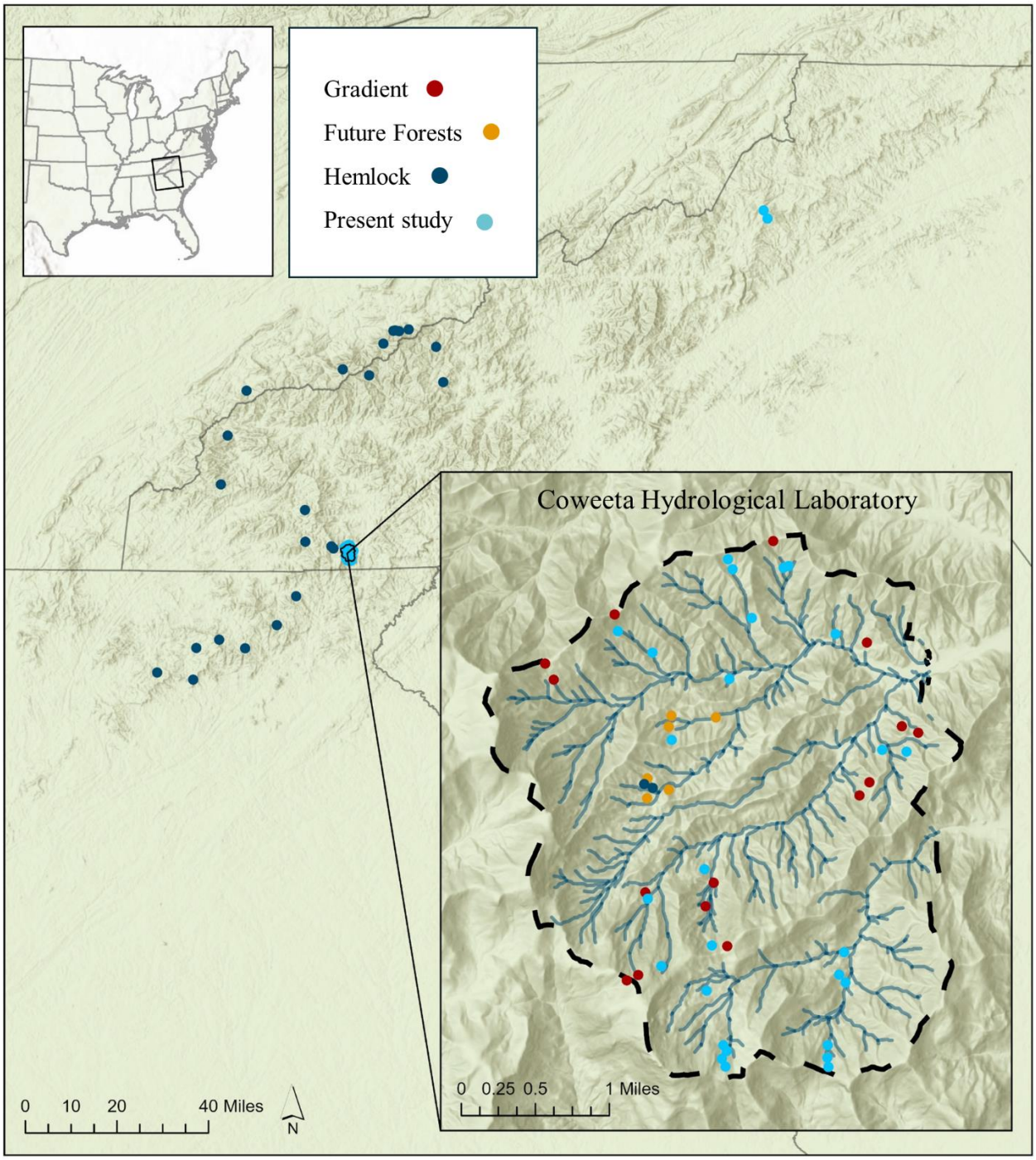

Figure 2.1 Study sites across the southern Blue Ridge Mountains and Coweeta Hydrological Laboratory. Sites outside of Coweeta have 15 plots each except for two sites near Grandfather Mountain, NC which have three plots each. Sites within Coweeta have two to six plots each.

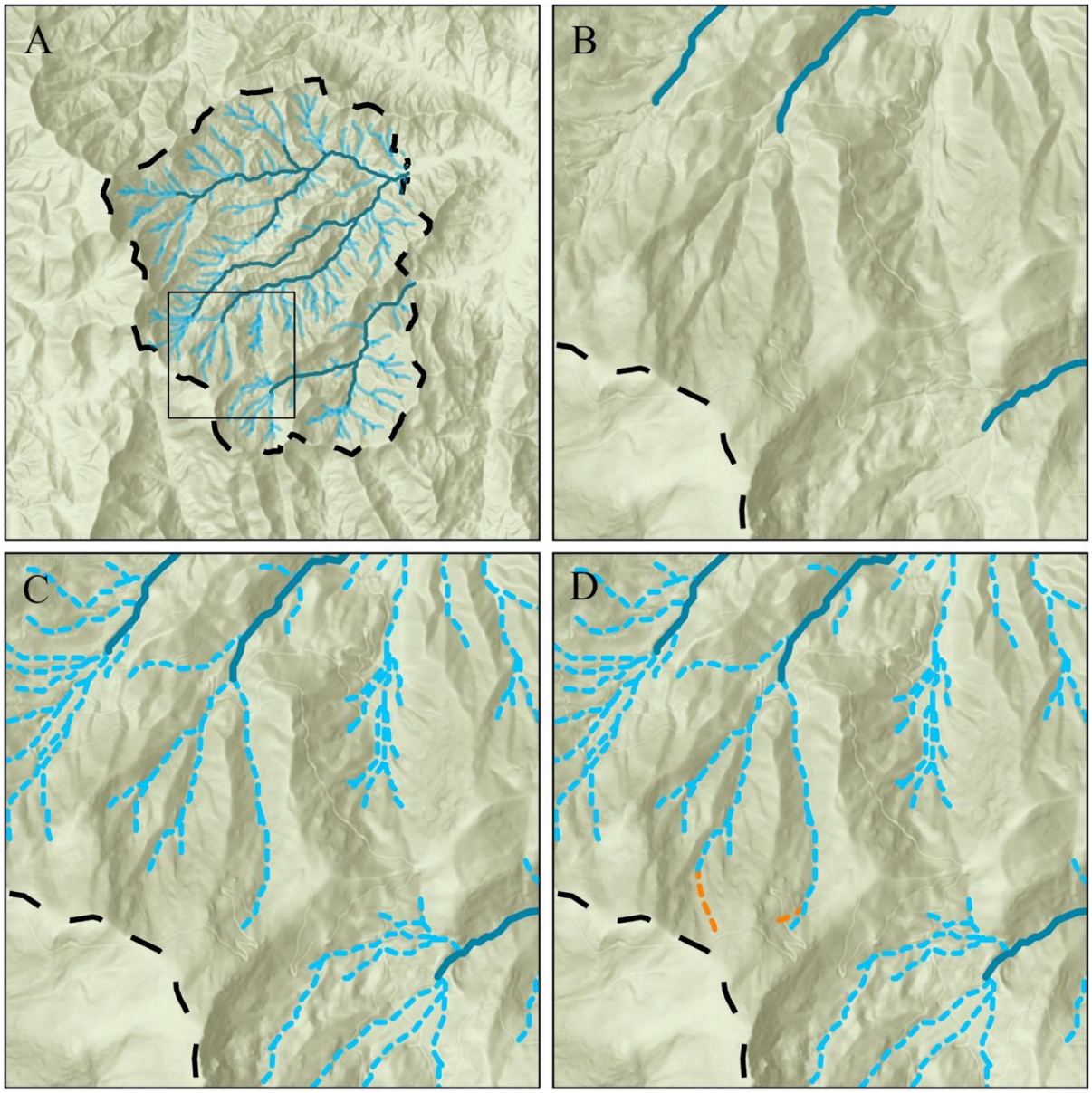

Figure 2.2 Perennial (B), ephemeral (C), and extended ephemeral (D) stream layers at Coweeta Hydrological Laboratory (A). Dark solid lines represent the extent of perennial streams, dotted light blue lines represent the extend of seasonal and ephemeral streams, and the orange dotted lines are seasonal streams we delineated by hand.

CHAPTER 3

RESULTS

We captured a total of 13,808 salamanders during the 3,949 individual plot surveys made from 2016 to 2023. Of all the salamanders observed, 79.6% were fully terrestrial species of "woodland salamanders" in the genus *Plethodon* (75.7%) and direct developing *Desmognathus* spp. (3.9%). The remaining 22.9% of salamanders were stream or pond-breeding species. Stream-breeding species were Blue Ridge Two-Lined salamanders (*Eurycea wilderae*, 6.6%), Mountain Dusky salamanders (*Desmognathus* spp. 12.2%), and larger stream-breeding salamanders (*Desmognathus* spp. *Gyrinophilus porphyriticus*, and *Pseudotriton ruber*; 1.7%). Pond-breeding salamanders were juvenile Eastern newts (*Notophthalmus viridescen;* 0.01%), and 0.01% of salamanders observed were unidentified (most often because of their depth within a burrow).

Trace plots and the Gelman-Rubin statistic ($\hat{R} < 1.1$) indicated successful chain convergence. Bayesian p-values on survey level counts of both taxa were close to 0.5, indicating good model fit (Table 3.1). Scatterplots of the discrepancy values used to calculate Bayesian p-values did not deviate far from a one-to-one line (a well fit model with a Bayesian p-value close to 0.5 would scatter evenly around the one-to-one line). Scatterplots of discrepancy values can be found in *Goodness of Fit* in Appendix D. The median chi-squared p-value on pass level counts for both taxa was approximately 0.4 (range: 0.015 – 0.951) suggesting that most of our observed counts matched expected counts adequately (Table 3.1). Only 2 % of our counts were poorly fit (below 0.05).

Model validation showed that when fit to Mountain Dusky counts, the model's mean absolute predictive error was between 0.008 and 0.019 individuals for each pass (Table 3.2). Since

average Mountain Dusky counts ranged from 0.081 to 0.174 individuals per pass, this means that on average the model over- or underestimated counts by 14%. When fit to Two-Lined counts, mean absolute predictive error was between 0.064 and 0.088 individuals for each pass. Average Two-Lined counts ranged from 0.081 to 0.174 individuals per pass, meaning that on average the model over- or under-estimated counts by 68%.

Parameter estimates were consistent with our hypotheses. We found a positive effect of elevation, a positive effect of northness, and a negative effect of stream distance on the abundance of both taxa, although the effect of elevation on the abundance of Two-Lined salamanders was weaker with the 95% credible intervals overlapping zero (Table 3.3). The effect of the interaction between the effect of elevation and the effect of stream distance was positive, indicating that the effect of stream distance declines with increasing elevation (Figures 3.1). In other words, as elevation increases, the predicted abundance of salamanders is greater at farther distances from streams and this effect is greater on north compared to south facing slopes (Figure 3.2).

The parameter estimates on the observation processes were also consistent with our hypotheses. Vapor pressure deficit had a negative effect and prior precipitation had a positive effect on salamander surface availability for capture (Table 3.3). The amount of vegetation cover below eye level had no effect on conditional capture probability of Mountain Dusky salamanders but had a positive effect on conditional capture of Blue Ridge Two-Line salamanders (Table 3.3).

Table 3.1 Bayesian p-values and chi-squared p-values for the Robust and Depletion observation processes fit to Mountain Dusky and Blue Ridge Two-Lined counts.

	Mountain Dusky Species	**Blue Ridge Two-Lined**
Robust observation process		
Survey counts $(y.r_k)$	0.541	0.519
Depletion observation process		
Survey counts (n_k)	0.595	0.667
Pass counts $\left(y.d_{k,1-4}\right)$	0.428	0.417
Pass counts range	0.018-0.951	0.015-0.927
Percent poorly fit pass counts	0.022	0.027

Table 3.2 Average counts per pass and mean absolute error per pass.

	Mountain Dusky Species	Blue Ridge Two-Lined
Average count		
Pass-1	0.127	0.174
Pass-2	0.101	0.119
Pass-3	0.085	0.100
Pass-4	0.083	0.081
Mean absolute error		
Pass-1	0.019	0.088
Pass-2	0.015	0.072
Pass-3	0.012	0.064
Pass-4	0.010	0.081

Table 3.3 Parameter estimates and Bayesian credible intervals from integrated abundance, availability, and detection (e.g. conditional capture probability) models for the two focal taxa. Estimates of abundance, availability, and detection are on the log and logit scale.

	Mountain Dusky Species			**Blue Ridge Two-Lined**		
	Mean	**2.5%**	**97.5**	**Mean**	**2.5%**	**97.5**
Abundance	12.527	0.004	95.983	3.158	0.312	12.273
Intercept	3.226	0.407	5.989	3.893	2.238	5.512
Elevation	1.719	1.322	2.133	0.131	-0.088	0.359
Distance	-1.797	-2.389	-1.290	-0.385	-0.629	-0.158
Elevation × Distance	0.754	0.373	1.201	0.193	-0.012	0.442
Northness	0.313	0.043	0.617	0.158	-0.008	0.330
Availability	0.006	0.000	0.059	0.008	0.001	0.034
Intercept	-6.468	-7.068	-5.433	-4.961	-5.267	-4.634
VPD	-0.572	-0.665	-0.479	-0.438	-0.553	-0.314
Precipitation	0.064	-0.023	0.163	0.136	0.064	0.218
Detection	0.134	0.016	0.462	0.157	0.009	0.615
Intercept	-2.232	-2.778	-1.632	-2.563	-3.121	-1.943
Vegetation	0.000	-0.233	0.234	0.203	0.046	0.366

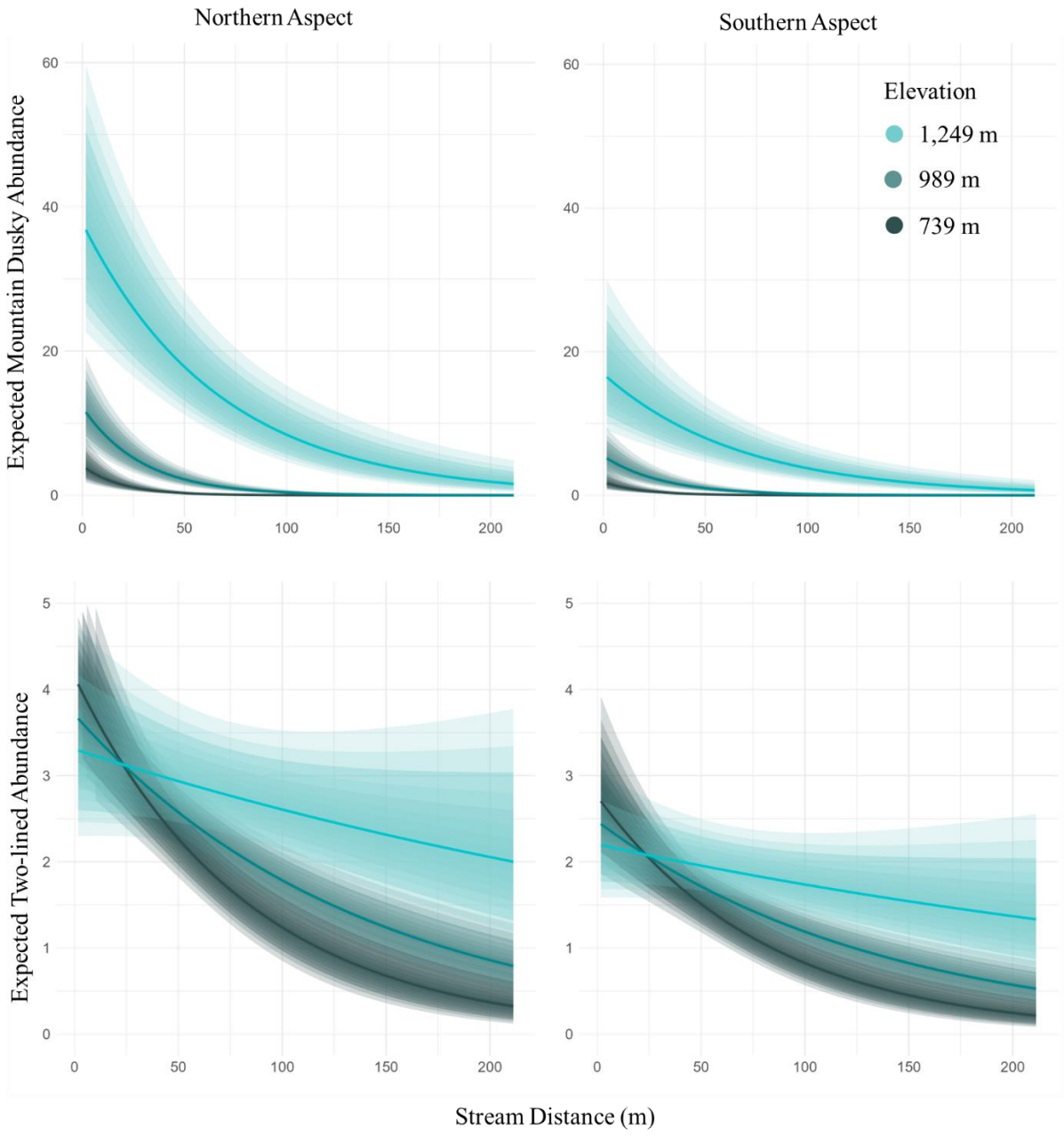

Figure 3.1 The predicted abundance of Mountain Dusky and Blue Ridge Two-Lined salamanders per 1 m² at 1,249 m, 989 m, and 739 m elevation on north and south facing hillslopes.

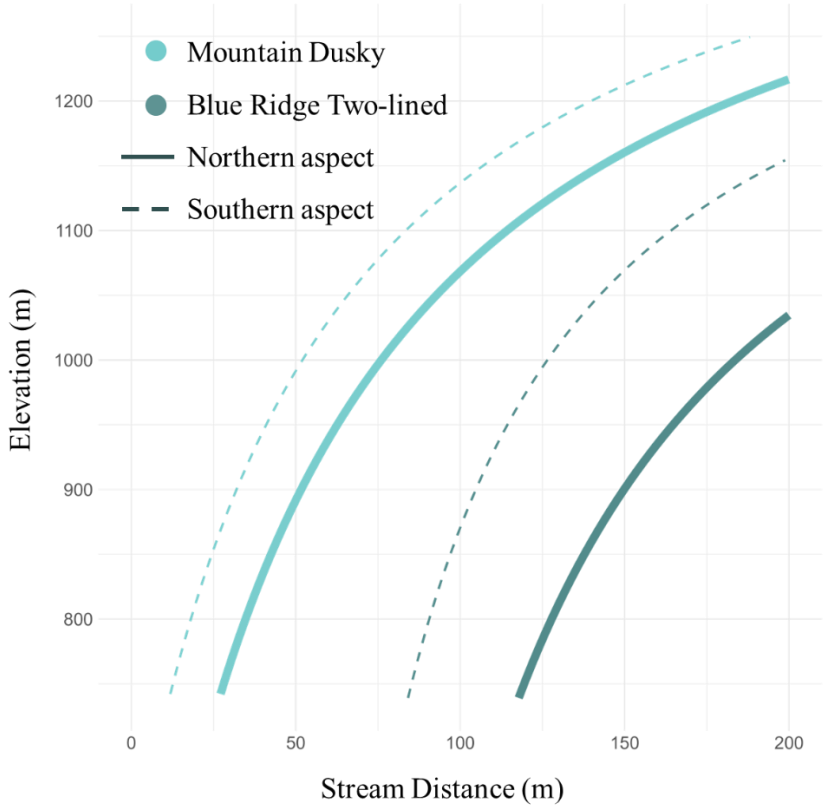

Figure 3.2 Distance at which the expected abundance of Mountain Dusky and Blue Ridge Two-Lined salamanders drops below 1 salamander per 1m² on north and south facing hillslopes.

CHAPTER 4

DISCUSSION

As predicted, we found that stream-breeding plethodontid abundance decreased with stream distance and that the rate at which their abundance decreased slowed with elevation and northness, mirroring our understanding of the local hydroclimate and hillslope hydrology. For Mountain Dusky salamanders, abundance declined with stream distance and increased with elevation such that, for a given distance from a stream, abundance increased with elevation and northness (Figure 3.1). Abundance estimates for Blue Ridge Two-Lined salamanders also followed this general pattern but were constant within the first 25 to 50 m from a stream regardless of elevation or aspect and then declined rapidly with increasing stream distance at lower elevations while remaining relatively constant at higher elevations (Figure 3.1).

Life history and microhabitat use mediate patterns of abundance

The differences we observed across our two focal taxa may reflect differences in their life histories and microhabitat use (Gould and Peterman, 2021). Both Mountain Dusky and Blue Ridge Two-Lined salamanders move between terrestrial uplands and aquatic nesting or overwintering sites, but the two taxa differ markedly in nest location and larval period. Mountain Dusky salamanders are well adapted to seasonal surface waters. Females nest immediately adjacent to but not within the flow of water under cover objects (Lannoo, 2005; Tilley, 1973) or embedded within the hyporheic zone of streams or seeps in small cavities or interstitial spaces (Keen & Orr, 1980; Tilley, 1973). Once hatched, larval Mountain Dusky Salamanders can metamorphose in 2 to 10-months (Bruce, 1989; Huheey & Brandon, 1973; Tilley, 1973). In contrast, Blue Ridge Two-Lined salamanders are most frequently observed nesting beneath the

cover of rocks or logs submerged in the water column of perennial streams (King, 1939; Lannoo, 2005) where larvae will remain for 1 to 3 years before metamorphosing (Bruce, 1982; Hudson, 1955; Petranka, 1984; Voss, 1993).

These differential adaptations to water permanence may underlie the differences we observe in Mountain Dusky and Blue Ridge Two-Lined salamander abundance. The same elevational patterns of precipitation and temperature that relax soil moisture gradients can also increase drainage density (Dunne et al., 1975; Hewlett & Hibbert, 1967); however, the flow in these headwater streams is often seasonal or ephemeral (Datry et al., 2014). Therefore, this increase in surface water density likely does not confer an increase in nesting habitat for Blue Ridge Two-Lined salamanders. It does, however, increase the density of nesting locations for Mountain Dusky salamanders. This means that as elevation increases Mountain Dusky salamanders have increased access to aquatic habitats for nesting and terrestrial habitats for foraging.

Behavior mediates detection

We had expected increased vegetation coverage to decrease an observer's ability to detect a salamander. Analysis of *Plethodon* spp. abundances on the same plots from the same surveys found a clear negative effect of vegetation cover on *Plethodon* conditional capture probability (Maerz et al. *in prep*). However, our results show that an observer was more likely to detect a Blue Ridge Two-Lined salamander in a plot with greater vegetation coverage than a plot with less vegetation, and that vegetation had little to no effect on the conditional capture probability of Mountain Dusky salamanders (Table 3.3). These differences may be a product of the species' behaviors. All three taxa routinely climb vegetation when conditions are favorable, but Blue Ridge Two-Lined salamanders are more likely to be observed climbing than Mountain Dusky or *Plethodon* salamanders (Hairston, 1949; LeGros, 2013; Mcentire, 2018). We suspect these

behavioral differences underlie the estimated effects of vegetation on conditional capture probability for each salamander group with vegetation cover having a negative effect on conditional capture probability of the more ground dwelling species and having a positive effect on species with a greater propensity to climb. It is possible that other factors such as color or body size also affect the detection of our two focal taxa. Howard (2018) showed that *Plethodon* capture probability declined with body size and it seems intuitive that observers may more readily detect bright yellow, Blue Ridge Two-Lined salamanders than cryptically mottled, Mountain Dusky salamanders. However, if the differences we observed in their detection were solely due to their coloration or body size we would expect to see differences in the overall detection probability of the two species, rather than differences in the effect of vegetation coverage.

Limitations

Our abundance estimates had relatively high uncertainty. This may be due to the fact that the multinomial distribution used to estimate conditional capture probability assumes that we can effectively deplete the population, meaning that fewer salamanders are observed with each pass. While average salamander counts did typically decrease from pass one to pass four, most surveys produced counts of one or zero salamanders. This means that counts observed during a typical survey could not show a clear pattern of depletion across passes. Nevertheless, our model was well fit to the error structure of our data and our observed counts (Table 3.1), so we believe our inferences are robust.

Ecosystem implications

Amphibians are believed to be important in the transport of energy and matter between terrestrial and aquatic habitats (Capps et al., 2015; Fritz et al., 2019; Regester et al., 2006). The annual

input of amphibian eggs and the mortality of young larvae can provide substantial amounts of high-quality, labile nutrients to freshwater ecosystems (Regester et al., 2006). Stream-breeding salamanders are thought to play a particularly important role in the transport of biomass and nutrients between terrestrial and freshwater stream ecosystems (Davic and Welsh, 2004). Our results indicate that this transport is substantially greater at higher elevations and more northern facing hillslopes where climates are wetter and cooler. This means that salamander-mediated transport across the aquatic-terrestrial interface is both greater and more broadly distributed at higher elevations and on northern facing hillslopes where wetter, cooler climates relax soil moisture gradients.

These stream breeding salamanders may be particularly important regarding the transport of phosphorus from terrestrial to aquatic habitats. The productivity of forested headwater stream ecosystems in Southern Appalachia is substantially limited by phosphorus availability (Webster et al., 2006). As vertebrates, stream-breeding salamanders have a relatively high phosphorus content and represent relatively large standing stocks of phosphorus in low order Southern Appalachian streams (Milanovich et al., 2015).

Management implications

Our results highlight the importance of ephemeral and seasonal (e.g. intermittent) streams, which often enjoy less protection than perennial streams. Much of the area we studied in southern Appalachia is public land managed by the USFS under the Final Nantahala-Pisgah Forest Management Plan. This 10–15-year plan, set in place in 2023, requires 100 ft buffers on perennial streams and 50 ft buffers on intermittent or seasonal streams, regardless of elevation (USFS, 2023). These buffers are largely intended to reduce the transport of silt and other runoff into streams but are also valued as a means to protect aquatic wildlife, including salamanders

(Peterman & Semlitsch, 2009). Our results suggest that, to protect a reasonable portion of stream-breeding salamander populations and their contributions to stream ecosystem processes, the size of riparian buffers should vary spatially, with increasing buffer sizes at higher elevations (Figure 3.2). This will be particularly important for streams on north-facing hillslopes, though we recognize varying buffer widths based on aspect would be challenging to incorporate into regulation. We note that densities of low order streams can be high at high elevations; so, expanding buffer widths to accommodate the broader terrestrial spatial distributions of salamanders could functionally eliminate timber harvest at high elevations. Therefore, an alternative approach is to set aside some high elevation areas and allow other drier sites or sites with lower stream densities to be used for timber rather than rely on uniform forest buffer distances across all sites.

The Final Nantahala-Pisgah Forest Management Plan strives to maintain the integrity of ephemeral streams but does not explicitly protect them. The Plan defines ephemeral streams as watercourses that "are always above the water table," "have short periods of flow in direct response to precipitation or snowmelt runoff," and have enough energy to remove leaf litter, organic matter, and soil down to mineral soil." They further qualify these streams are watercourses that "do not contain riparian vegetation, fish, or aquatic insects with multiple-year larval life cycle phases." Presumably these biological indicators serve to discern an ephemeral stream from an intermittent or seasonal stream. We commend the Forest Service for their use of such ecologically relevant indicators but encourage them to add stream-breeding salamanders to their list. One of our most abundant study sites at Coweeta (in Watershed 36 near Big-spring Gap) is near a watercourse that meets the Forest Service's definition of an ephemeral stream; however, the abundance of Mountain Dusky salamanders found near it indicates that the

subsurface maintains a flow sufficient for their reproduction. Adding stream-breeding salamanders to the list of biological indicators could help the Forest Service identify seasonal subsurface flows that are biologically and hydrologically connected to adjacent uplands and downstream networks.

References

Baxter, C. V., Fausch, K. D., & Carl Saunders, W. (2005). Tangled webs: Reciprocal flows of invertebrate prey link streams and riparian zones. *Freshwater Biology*, *50*(2), 201–220. https://doi.org/10.1111/j.1365-2427.2004.01328.x

Bradke, D. R. (2023). *Population Modeling to Inform Monitoring and Management of Herpetofauna in the Southeastern United States* [Ph.D. Dissertation]. University of Georgia.

Bruce, R. C. (1982). Egg-Laying, Larval Periods and Metamorphosis of Eurycea bislineata and E. junaluska at Santeetlah Creek, North Carolina. *Copeia*, *1982*(4), 755–762. https://doi.org/10.2307/1444083

Bruce, R. C. (1989). Life History of the Salamander Desmognathus monticola, with a Comparison of the Larval Periods of D. monticola and D. ochrophaeus. *Herpetologica*, *45*(2), 144–155.

Camp. (2024). Assortment of Dusky Salamanders along Moisture Gradients in Multispecies Assemblages: Revisiting the Ideas. *Herpetologica*. https://doi.org/10.1655/Herpetologica-D-23-00031.1

Capps, K. A., Berven, K. A., & Tiegs, S. D. (2015). Modelling nutrient transport and transformation by pool-breeding amphibians in forested landscapes using a 21-year dataset. *Freshwater Biology*, *60*(3), 500–511. https://doi.org/10.1111/fwb.12470

Connette, G. M., Osbourn, M. S., & Peterman, W. E. (2016). The Distribution of a Stream-breeding Salamander, Desmognathus ocoee, in Terrestrial Habitat Suggests the Ecological Importance of Low-order Streams. *Copeia*, *104*(1), 149–156. https://doi.org/10.1643/OT-14-215

Connette, G. M., & Semlitsch, R. D. (2013). Life history as a predictor of salamander recovery rate from timber harvest in southern appalachian forests, USA. *Conservation Biology: The Journal of the Society for Conservation Biology*, *27*(6), 1399–1409. https://doi.org/10.1111/cobi.12113

Crawford, J. A., & Semlitsch, R. D. (2007). Estimation of Core Terrestrial Habitat for Stream-Breeding Salamanders and Delineation of Riparian Buffers for Protection of Biodiversity. *Conservation Biology*, *21*(1), 152–158. https://doi.org/10.1111/j.1523-1739.2006.00556.x

Crawford, J. A., & Semlitsch, R. D. (2008). Abiotic factors influencing abundance and microhabitat use of stream salamanders in southern Appalachian forests. *Forest Ecology and Management*, *255*(5), 1841–1847. https://doi.org/10.1016/j.foreco.2007.12.005

Datry, T., Larned, S. T., & Tockner, K. (2014). Intermittent Rivers: A Challenge for Freshwater Ecology. *BioScience*, *64*(3), 229–235. https://doi.org/10.1093/biosci/bit027

Dunne, T., Moore, T., & Taylor, C. (1975). Recognition and Prediction of Runoff-Producing Zones in Humid Regions. *Hydrol Sci BULL Sci Hydrol*, *20*.

Feder, M. E. (1983). Integrating the Ecology and Physiology of Plethodontid Salamanders. *Herpetologica*, *39*(3), 291–310.

Ford, W. M., Menzel, M. A., & Odom, R. H. (2002). Elevation, Aspect, and Cove Size Effects on Southern Appalachian Salamanders. *Southeastern Naturalist*, *1*(4), 315–324.

Fritz, K. A., Whiles, M. R., & Trushenski, J. T. (2019). Subsidies of long-chain polyunsaturated fatty acids from aquatic to terrestrial environments via amphibian emergence. *Freshwater Biology*, *64*(5), 832–842. https://doi.org/10.1111/fwb.13266

Gade, M. R., Connette, G. M., Crawford, J. A., Hocking, D. J., Maerz, J. C., Milanovich, J. R., & Peterman, W. E. (2020). Predicted alteration of surface activity as a consequence of climate change. *Ecology*, *101*(11). https://doi.org/10.1002/ecy.3154

Gelman, A., Carlin, J. B., Stern, H. S., Dunson, D. B., Vehtari, A., & Rubin, D. B. (2021). *Bayesian Data Analysis Third edition (with errors fixed as of 15 February 2021)*.

Gelman, A., & Rubin, D. B. (1992). Inference from Iterative Simulation Using Multiple Sequences. *Statistical Science*, *7*(4), 457–472. https://doi.org/10.1214/ss/1177011136

Griffith, G., Omernick, J., Comstock, J., Schfale, M., McNab, W., Lenat, D., Glover, J., & Shelburne, V. (2002). *Ecoregions of North Carolina and South Carolina*.

Hairston, N. G. (1949). The Local Distribution and Ecology of the Plethodontid Salamanders of the Southern Appalachians. *Ecological Monographs*, *19*(1), 47–73. https://doi.org/10.2307/1943584

Hairston, N. G. (1987). *Community Ecology and Salamander Guilds*. Cambridge University Press.

Head, L. (2020). *Short-Term Responses of Plethodontid Salamanders to the Restoration of Prescribed Fire within the Coweeta Hydrologic Laboratory* [Senior Thesis]. University of Georgia.

Helvey, J. D., Hewlett, J. D., & Douglass, J. E. (1972). Predicting Soil Moisture in the Southern Appalachians. *Soil Science Society of America Journal*, *36*(6), 954–959. https://doi.org/10.2136/sssaj1972.03615995003600060033x

Hewlett, J. D., & Hibbert, A. R. (1967). Factors affecting the response of small watersheds to precipitation in humid areas. *Pergamon Press*.

Hocking, D. J., Crawford, J. A., Peterman, W. E., & Milanovich, J. R. (2021). Abundance of montane salamanders over an elevational gradient. *Ecology and Evolution*, *11*(3), 1378–1391. https://doi.org/10.1002/ece3.7142

Howard, J. S. (2018). *Modeling the Effects of Precipitation on Salamander Demography for Conservation Planning* [Ph.D. Dissertation]. University of Georgia.

Hudson, R. G. (1955). Observations on the Larvae of the Salamander Eurycea bislineata bislineata. *Herpetologica*, *11*(3), 202–204.

Huheey, J. E., & Brandon, R. A. (1973). Rock-Face Populations of the Mountain Salamander, Desmognathus Ochrophaeus, In North Carolina. *Ecological Monographs*, *43*(1), 59–77. https://doi.org/10.2307/1942159

Hwang, T., Band, L. E., Miniat, C. F., Vose, J. M., Knoepp, J. D., Song, C., & Bolstad, P. V. (2020). Climate Change May Increase the Drought Stress of Mesophytic Trees Downslope With Ongoing Forest Mesophication Under a History of Fire Suppression. *Frontiers in Forests and Global Change*, *3*, 17. https://doi.org/10.3389/ffgc.2020.00017

Hwang, T., Band, L. E., Vose, J. M., & Tague, C. (2012). Ecosystem processes at the watershed scale: Hydrologic vegetation gradient as an indicator for lateral hydrologic connectivity of headwater catchments. *Water Resources Research*, *48*(6). https://doi.org/10.1029/2011WR011301

Keen, W. H., & Orr, L. P. (1980). Reproductive Cycle, Growth, and Maturation of Northern Female Desmognathus ochrophaeus. *Journal of Herpetology*, *14*(1), 7–10. https://doi.org/10.2307/1563868

Kellner, K., & Meredith, M. (2024). *jagsUI: A Wrapper Around "rjags" to Streamline "JAGS" Analyses* (1.6.2) [Computer software]. https://cran.r-project.org/web/packages/jagsUI/index.html

King, W. (1939). A Survey of the Herpetology of Great Smoky Mountains National Park. *The American Midland Naturalist*, *21*(3), 531–582. https://doi.org/10.2307/2420516

Konrad Ii, C. E. (1996). Relationships Between Precipitation Event Types and Topography in the Southern Blue Ridge Mountains of the Southeastern Usa. *International Journal of Climatology*, *16*(1), 49–62. https://doi.org/10.1002/(SICI)1097-0088(199601)16:1<49::AID-JOC993>3.0.CO;2-D

Lannoo, M. (2005). Amphibian Declines: The Conservation Status of United States Species. *Amphibian Declines: The Conservation Status of United States Species*. https://doi.org/10.1525/california/9780520235922.001.0001

LeGros, D. L. (2013). Plant Climbing in the Northern Two-Lined Salamander, Eurycea bislineata, in Algonquin Provincial Park, Ontario. *The Canadian Field-Naturalist*, *127*(1), Article 1. https://doi.org/10.22621/cfn.v127i1.1411

Leroux, S. J., & Loreau, M. (2008). Subsidy hypothesis and strength of trophic cascades across ecosystems. *Ecology Letters*, *11*(11), 1147–1156. https://doi.org/10.1111/j.1461-0248.2008.01235.x

Marcarelli, A., Baxter, C., Mineau, M., & Hall, R. (2011). Quantity and quality: Unifying food web and ecosystem perspectives on the role of resource subsidies in freshwaters. *Ecology*, *92*, 1215–1225. https://doi.org/10.1890/10-2240.1

Mcentire, K. D. (2018). *Integration of Behavior Into Biophysical Models to Estimate Salamander Sensitivity to Climate and Midstory Forest Management* [Ph.D. Dissertation]. University of Georgia.

Milanovich, J. R., Maerz, J. C., & Rosemond, A. D. (2015). Stoichiometry and estimates of nutrient standing stocks of larval salamanders in Appalachian headwater streams. *Freshwater Biology*, *60*(7), 1340–1353. https://doi.org/10.1111/fwb.12572

Organ, J. A. (1961). Studies of the Local Distribution, Life History, and Population Dynamics of the Salamander Genus Desmognathus in Virginia. *Ecological Monographs*, *31*(2), 189–220. https://doi.org/10.2307/1950754

Peterman, W. E., & Semlitsch, R. D. (2009). Efficacy of riparian buffers in mitigating local population declines and the effects of even-aged timber harvest on larval salamanders. *Forest Ecology and Management*, *257*(1), 8–14. https://doi.org/10.1016/j.foreco.2008.08.011

Petranka, J. W. (1984). Ontogeny of the Diet and Feeding Behavior of Eurycea bislineata Larvae. *Journal of Herpetology*, *18*(1), 48–55. https://doi.org/10.2307/1563671

Petranka, J. W., & Murray, S. S. (2001). Effectiveness of Removal Sampling for Determining Salamander Density and Biomass: A Case Study in an Appalachian Streamside Community. *Journal of Herpetology*, *35*(1), 36–44. https://doi.org/10.2307/1566020

Petranka, J. W., & Smith, C. K. (2005). A functional analysis of streamside habitat use by southern Appalachian salamanders: Implications for riparian forest management. *Forest Ecology and Management*, *210*(1), 443–454. https://doi.org/10.1016/j.foreco.2005.02.040

Plummer, M. (2003). JAGS: A Program for Analysis of Bayesian Graphical Models using Gibbs Sampling. *3rd International Workshop on Distributed Statistical Computing (DSC 2003); Vienna, Austria*, *124*.

Polis, G. A., Anderson, W. B., & Holt, R. D. (1997). Toward an Integration of Landscape and Food Web Ecology: The Dynamics of Spatially Subsidized Food Webs. *Annual Review of Ecology, Evolution, and Systematics*, *28*(Volume 28, 1997), 289–316. https://doi.org/10.1146/annurev.ecolsys.28.1.289

Pollock, K. H. (1982). A Capture-Recapture Design Robust to Unequal Probability of Capture. *The Journal of Wildlife Management*, *46*(3), 752–757. https://doi.org/10.2307/3808568

Pyron, R. A., & Beamer, D. A. (2022a). Nomenclatural solutions for diagnosing 'cryptic' species using molecular and morphological data facilitate a taxonomic revision of the Black-bellied Salamanders (Urodela, Desmognathus 'quadramaculatus') from the southern Appalachian Mountains. *Bionomina*, *27*(1). https://doi.org/10.11646/bionomina.27.1.1

Pyron, R. A., & Beamer, D. A. (2022b). Systematics of the Ocoee Salamander (Plethodontidae: Desmognathus ocoee), with description of two new species from the southern Blue Ridge Mountains. *Zootaxa*, *5190*(2), 207–240. https://doi.org/10.11646/zootaxa.5190.2.3

Regester, K. J., Whiles, M. R., & Taylor, C. M. (2006). *Decomposition Rates of Salamander (Ambystoma Maculatum) Life Stages and Associated Energy and Nutrient Fluxes in Ponds and Adjacent Forest in Southern Illinois*. https://dx.doi.org/10.1643/0045-8511(2006)6[640:DROSAM]2.0.CO;2

Rivenbark, B. L., & Jackson, C. R. (2004). Average Discharge, Perennial Flow Initiation, and Channel Initiation—Small Southern Appalachian Basins1. *JAWRA Journal of the*

American Water Resources Association, *40*(3), 639–646. https://doi.org/10.1111/j.1752-1688.2004.tb04449.x

Rucker, L. E., Brown, D. J., Jacobsen, C. D., Messenger, K. R., Wild, E. R., & Pauley, T. K. (2021). A Guide to Sexing Salamanders in Central Appalachia, United States. *Journal of Fish and Wildlife Management*, *12*, 1–19. https://doi.org/10.3996/JFWM-20-042

Scaife, C. I., Duncan, J. M., Lin, L., Tague, C., Bell, C. D., & Band, L. (2021). Are spatial patterns of soil moisture at plot scales generalisable across catchments, climates, and other characteristics? A synthesis of synoptic soil moisture across the Mid-Atlantic. *Hydrological Processes*, *35*(9), e14313. https://doi.org/10.1002/hyp.14313

Schaub, M., & Kéry, M. (2022). Chapter 1—Introduction. In M. Schaub & M. Kéry (Eds.), *Integrated Population Models* (pp. 1–8). Academic Press. https://doi.org/10.1016/B978-0-12-820564-8.00013-0

Semlitsch, R. D., O'Donnell, K. M., & III..Thompson, F. R. (2014). Abundance, biomass production, nutrient content, and the possible role of terrestrial salamanders in Missouri Ozark forest ecosystems. *Canadian Journal of Zoology. 92: 997-1004.*, *92*, 997–1004. https://doi.org/10.1139/cjz-2014-0141

Subalusky, A. L., & Post, D. M. (2019). Context dependency of animal resource subsidies. *Biological Reviews*, *94*(2), 517–538. https://doi.org/10.1111/brv.12465

Tilley, S. G. (1973). Life Histories and Natural Selection in Populations of the Salamander Desmognathus Ochrophaeus. *Ecology*, *54*(1), 3–17. https://doi.org/10.2307/1934370

Vanni, M. (2002). Nutrient Cycling by Animals in Freshwater Ecosystems. *Annu. Rev. Ecol. Syst*, *33*, 341–370. https://doi.org/10.1146/annurev.ecolsys.33.010802.150519

Voss, S. R. (1993). Relationship between Stream Order and Length of Larval Period in the Salamander Eurycea wilderae. *Copeia*, *1993*(3), 736–742. https://doi.org/10.2307/1447235

Webster, J. R., Wallace, J. B., & Benfield, E. F. (2006). Organic Processes in stream of the Eastern United States. In *River and Stream Ecosytems of the World: With a New Introduction* (pp. 117–187). University of California Press.

APPENDIX A

PLOT AND SITE ATTRIBUTE DEREVATION

The following procedures were carried out in Arc Pro 3.2.2

Bring raw data into the Arc Project

1. **Add DEMs** to Arc Project.

   Eighteen 1/3 arc second (10m) DEM rasters from the National Map (apps.nationalmap.gov) were mosaiced together to create the DEM used to derive elevation, aspect, and the streamlines used to calculate stream distance. This mosaiced raster's native CS is NAD ’83.

   It was mosaiced by Jeff Hepinstall-Cymerman using the command below:

   arcpy.management.MosaicToNewRaster(r"'DEM 10 m 2023 mosaic attempts\USGS_13_n36w085_20220725.tif';'DEM 10 m 2023 mosaic attempts\USGS_13_n35w086_20220728.tif';'DEM 10 m 2023 mosaic attempts\USGS_13_n36w086_20220729.tif';'DEM 10 m 2023 mosaic attempts\USGS_13_n37w083_20220512.tif';'DEM 10 m 2023 mosaic attempts\USGS_13_n36w081_20130911.tif';'DEM 10 m 2023 mosaic attempts\USGS_13_n37w084_20181127.tif';'DEM 10 m 2023 mosaic attempts\USGS_13_n38w082_20230816.tif';'DEM 10 m 2023 mosaic attempts\USGS_13_n35w085_20230215.tif';'DEM 10 m 2023 mosaic attempts\USGS_13_n36w083_20220512.tif';'DEM 10 m 2023 mosaic attempts\USGS_13_n35w083_20230215.tif';'DEM 10 m 2023 mosaic attempts\USGS_13_n37w081_20210305.tif';'DEM 10 m 2023 mosaic attempts\USGS_13_n38w081_20230816.tif';'DEM 10 m 2023 mosaic

attempts\USGS_13_n38w080_20211229.tif';'DEM 10 m 2023 mosaic attempts\USGS_13_n37w082_20220512.tif';'DEM 10 m 2023 mosaic attempts\USGS_13_n37w080_20210305.tif';'DEM 10 m 2023 mosaic attempts\USGS_13_n36w082_20220512.tif';'DEM 10 m 2023 mosaic attempts\USGS_13_n36w084_20220725.tif';'DEM 10 m 2023 mosaic attempts\USGS_13_n35w084_20230215.tif'", r"D:\DEM\dem.gdb", "sapps10mdem2023GCS", 'GEOGCS["GCS_North_American_1983",DATUM["D_North_American_1983",SPHEROID["GRS_1980",6378137.0,298.257222101]],PRIMEM["Greenwich",0.0],UNIT["Degree",0.0174532925199433]]', "32_BIT_FLOAT", None, 1, "MAXIMUM", "FIRST")

2. **Add csv of plot coordinates** to the Arc Project

   Plot coordinates were recorded in the field using Avenza (store.avenza.com). The map used to record plot locations in the Avenza App was stored in the NAD ’83 GCS. Plot coordinates were exported from the app to csv.

3. **Add csv of site coordinates** to the Arc Project

   Site coordinates were not recorded in the field. Plots coordinates were averaged in the R environment to create site coordinates. One site, WS27R was broken into two sites for analysis because plots were spatially clustered in two locations far enough from one another to have significantly different site attributes (and potentially different effects on availability). Site coordinates were stored in csv format.

4. **Add XY data** to the Plots and Sites using the same coordinate system as the DEM, NAD ’83. Note, this is the same GCS used to record plot locations in Avenza.

Create attribute raster layers

5. Create a **Slope** raster using the Slope tool from the Spatial Analyst Toolbox; set the GCS and Mask to that of the DEM in the environment. Output slope measurements in degrees. No Z factor was provided. A default Z factor of 1 was used.

6. Create an **Aspect** raster using the Aspect tool from the Spatial Analyst Toolbox, set the output to radians, and in the environment, set the GCS and Mask to that of the DEM.

7. Create a **Hydro DEM** raster using the Fill Sinks tool from the ArcHydro Toolbox. No fill threshold or deranged polygon was provided. Use Is Sink Field was not checked.

8. Derive **Flow Direction** raster using the Flow Direction Tool from the ArcHydro Toolbox. No External Wall Polygon was provided.

9. Derive **Flow Accumulation** raster using the Flow Direction Tool from the ArcHydro Toolbox.

10. *Step ten was discarded from the final workflow.*

    Project the raster into the USA Contiguous Albers Equal Area Conic USGS. This does not require a transformation; the Nearest neighbor resampling technique is used. The output coordinate system is affirmed in the environment, and the extent is set to that of the original DEM. Reprojection changes the cell size from 9.25x9.25m to 10.5x10.5 meters, complicating later stream definition because areas must be recalculated.

    a. *The final stream layer produced from this projected layer produced many tiny segments rather than continuous lines, so projected streams were not used for analysis. See below for more details on this decision process.* *

11. Create a **raster of perennial streams** using the Define Streams Tool in the ArcHydro Toolbox. Perennial streams are defined by an accumulating area of 19 acres or 0.0768903 km² (Rivenbark and Jackson 2004). This value was entered into the Areas Sqkm stream field, which populated 692 cells to define a stream layer.

12. Create a **polyline of perennial streams** using the Stream to Feature tool in the Spatial Analyst Toolbox. This tool's inputs were the NAD83 perennial stream raster and the NAD83 flow direction raster.

13. Create a **raster of ephemeral streams** using the Define Streams Tool in the ArcHydro Toolbox. Ephemeral streams are defined by an accumulating area of 0.75 acres or 0.003035142 km², which was derived from iterative runs of this workflow. Stream layers were compared to the on-the-ground study sites. The most accurate layer was selected. This value was entered into the Areas Sqkm stream field, which populated 303 cells to define a stream layer.

14. Create a **polyline of ephemeral streams** using the Stream to Feature tool in the Spatial Analyst Toolbox. This tool's input was the NAD83 perennial stream raster and the NAD 83 flow direction raster.

15. **Extract values to points** using the Extract Multi Values to Points from the Spatial Analyst Toolbox.

16. **Derive the distance** to the nearest perennial and ephemeral streamline using the Near tool from the Spatial Analyst Toolbox. Set the method to geodesic and the units to meters. No other selections.

APPENDIX B

RANDOM FOREST MODEL OPTIMIZATION, FIT, AND EVALUATION

We fit three random forest models to interpolate missing relative humidity and air temperature values. Each model fit one type of missing value. The first fit (1) relative humidity where relative humidity was the only value missing. The second model fit (2) relative humidity where both relative humidity and air temperature were missing and the third fit (3) air temperature where both relative humidity and air temperature were missing.

For each model we used the 'rsample' package (v1.2.1; Frick et al., 2024) to create a hyper grid of tuning parameters for model training and the 'ranger' package (v0.16.0; Wright et al. 2023) to fit models following the steps below.

1. Subset data into subsets for training and prediction
2. Select optimal tuning parameters (using training data)
    a. Create a hyper grid of available parameters
        i. mtry and node size ranged from 1 to the number of covariates
        ii. sample sizes were 0.55, 0.63, 0.70, or 0.80
    b. Iteratively fit the model using the entire hyper grid space
    c. Join the out-of-bag root mean square error to the hyper grid
    d. Select the optimal tuning parameters out-of-bag root mean square error
3. Bootstrap 100 iterations of the model using the optimal tuning parameters to evaluate model performance (out-of-bag root mean squared error)

4. Train the model using the optimal tuning parameters

5. Assess variable importance

6. Predict missing values using the trained model

Each time we fit a model for parameter selection, training or prediction we used 500 trees and all of the available covariates including year, month, Julian date, start time, air temperature, relative humidity, site latitude, site elevation, site slope, site aspect, and site stream distance. The model fit to relative humidity excluded relative humidity from the covariate dataset and both models fit to data where both relative humidity and air temperature were missing excluded both of these missing values from covariate datasets.

Below we present the out-of-bag root mean square error (OOB RMSE), variable importance, and plots of predicted vs measured for each of the three models. For each model these values are presented for each site for which missing values were interpolated

Model 1. OOB RMSE

Interpolated relative humidity where relative humidity was the only value missing.

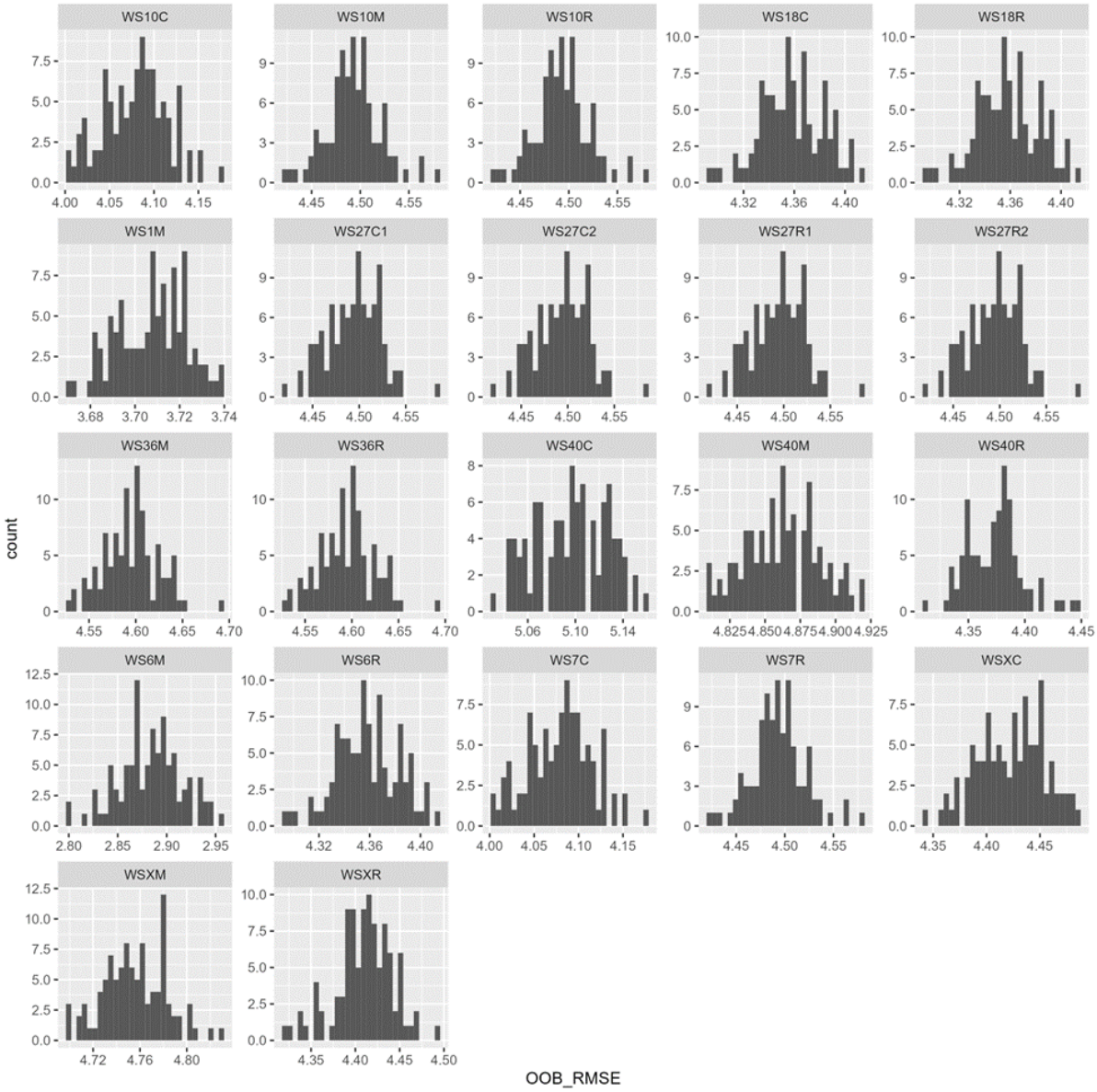

Model 1. Variable Importance

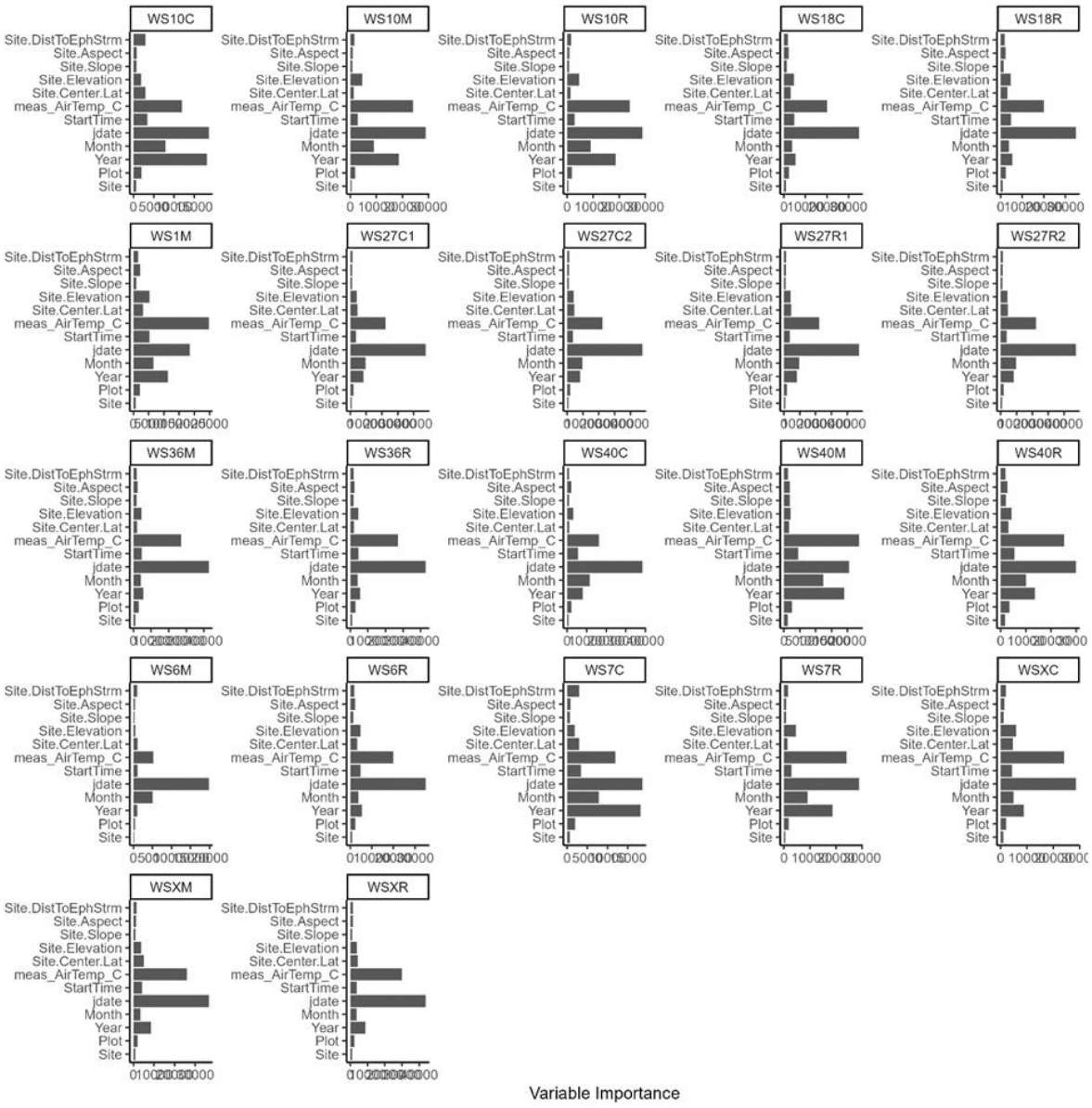

Model 1. Predicted vs. Measured

predicted (blue), measured (red)

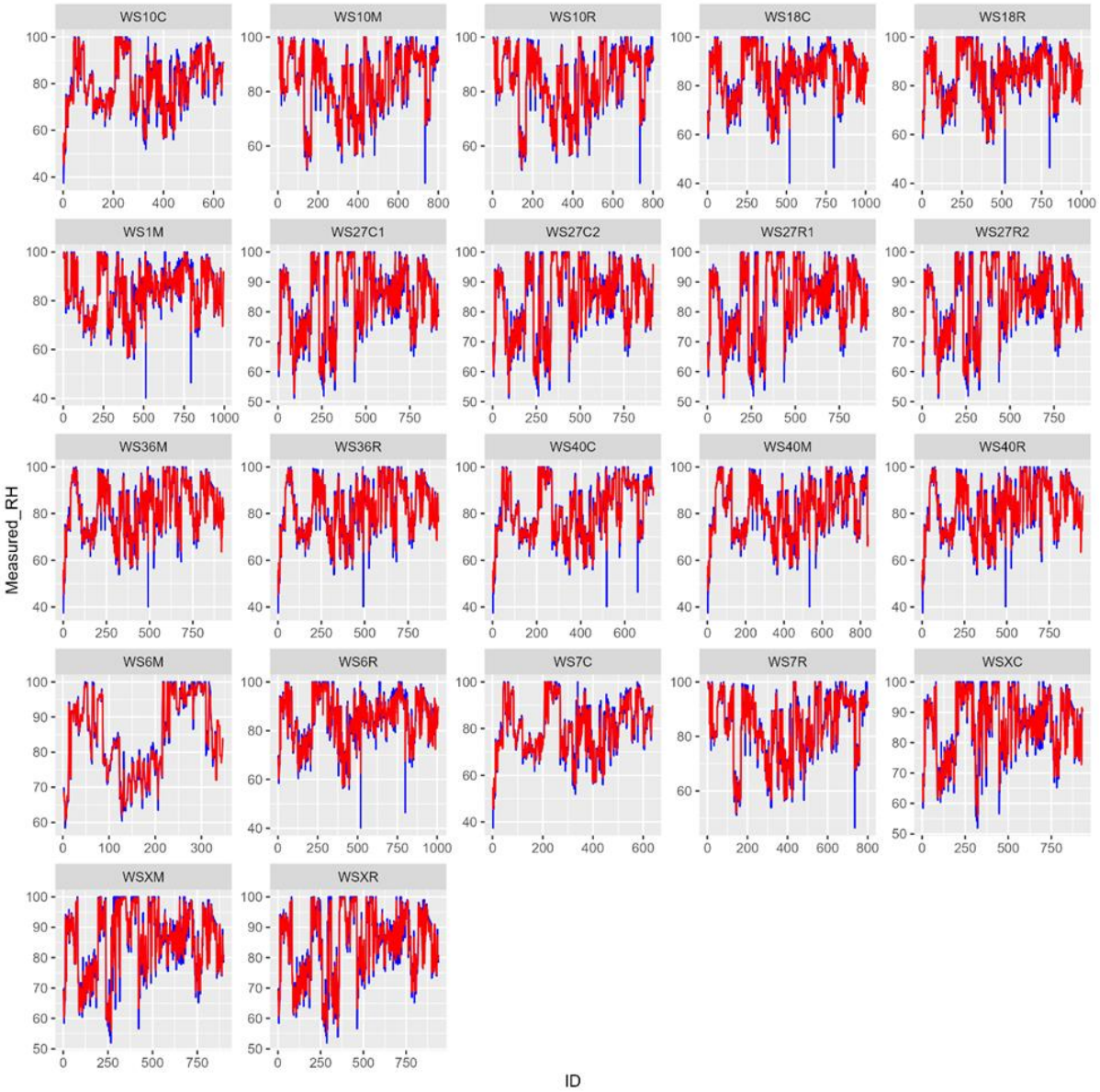

Model 2. OOB RMSE

Interpolated relative humidity where relative humidity and air temperature values were missing.

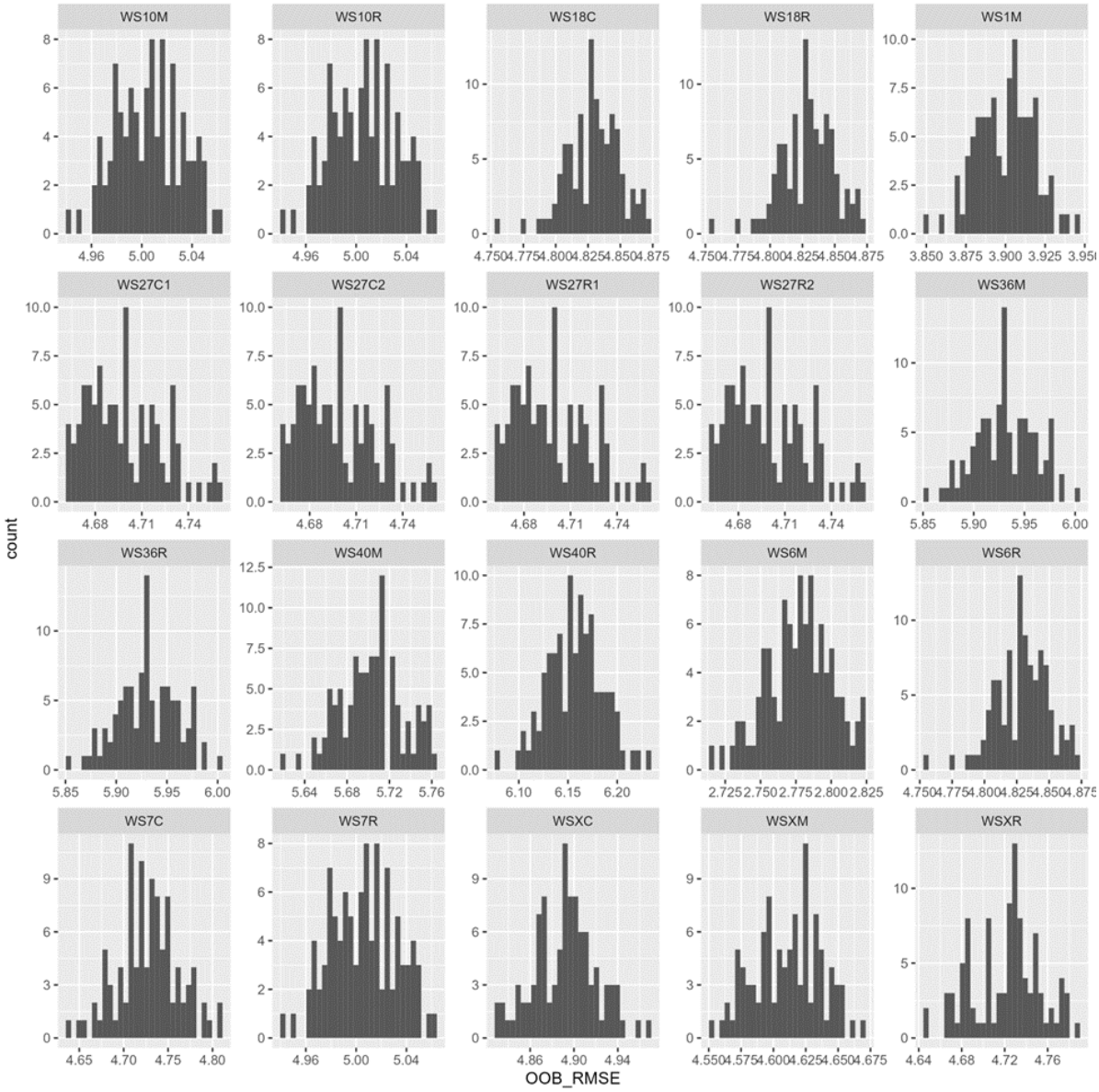

Model 2. Variable Importance

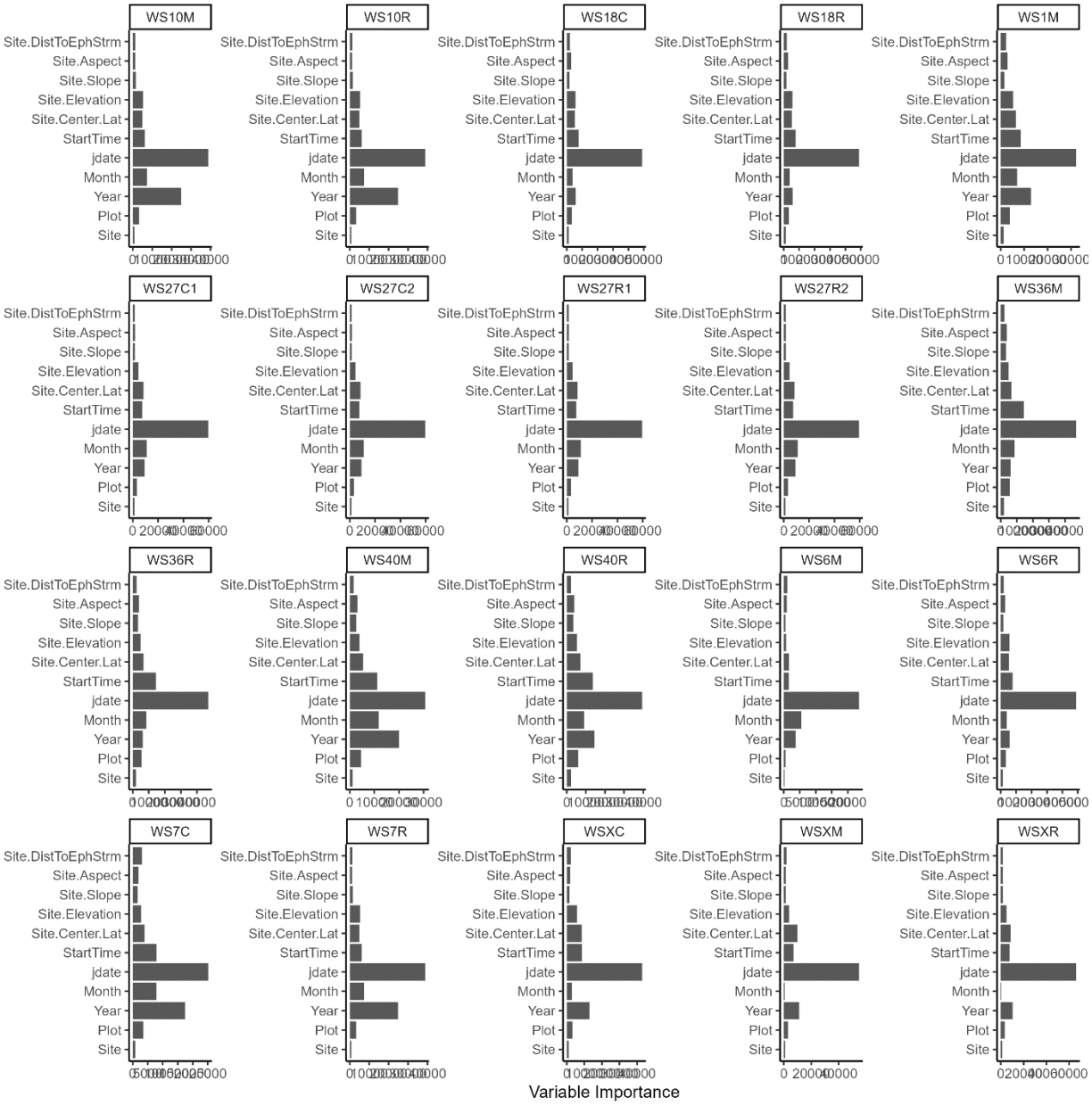

Model 2. Predicted vs. Measured

predicted (blue), measured (red)

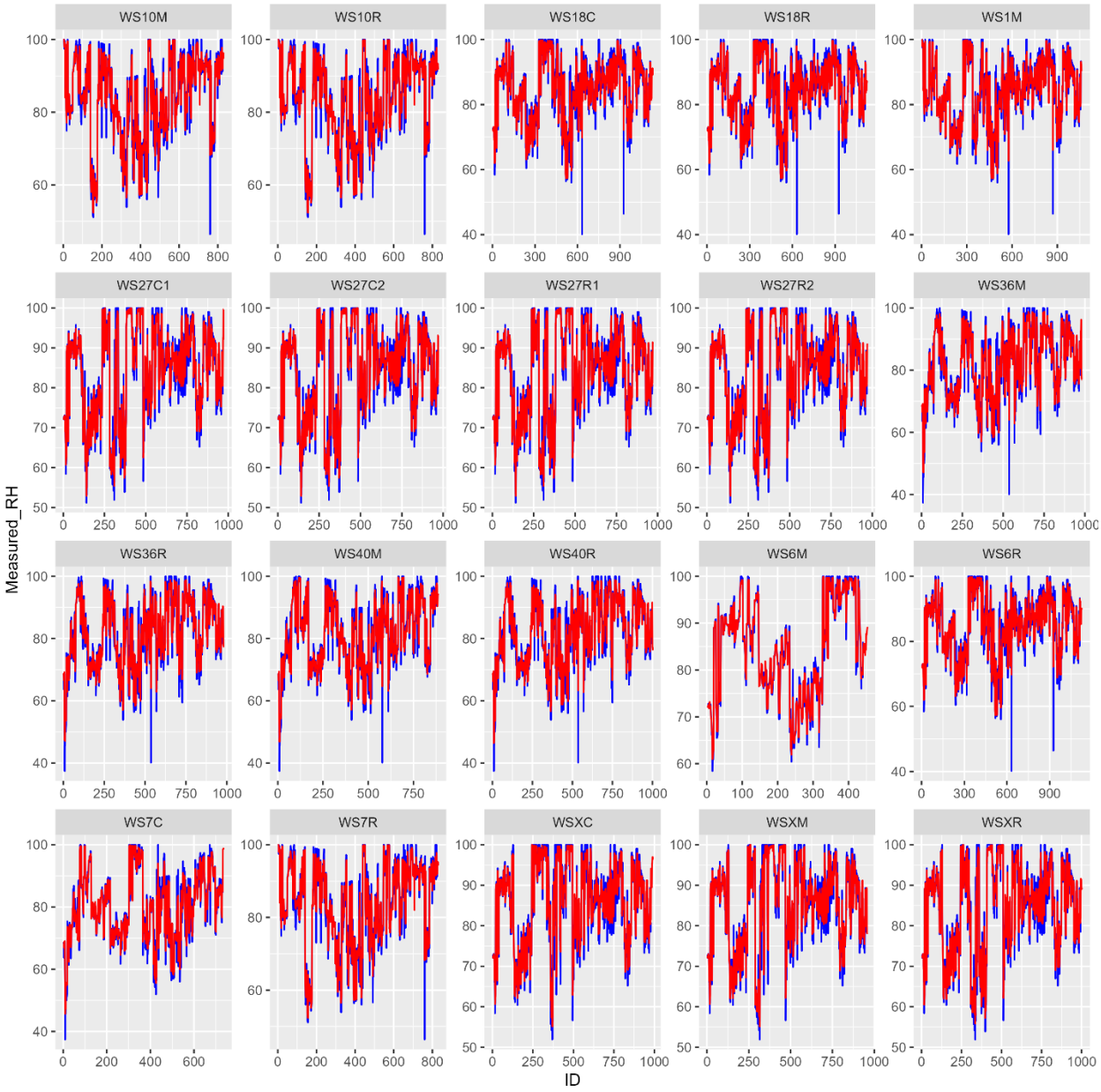

Model 3. OOB RMSE

Interpolated air temperature where relative humidity and air temperature values were missing.

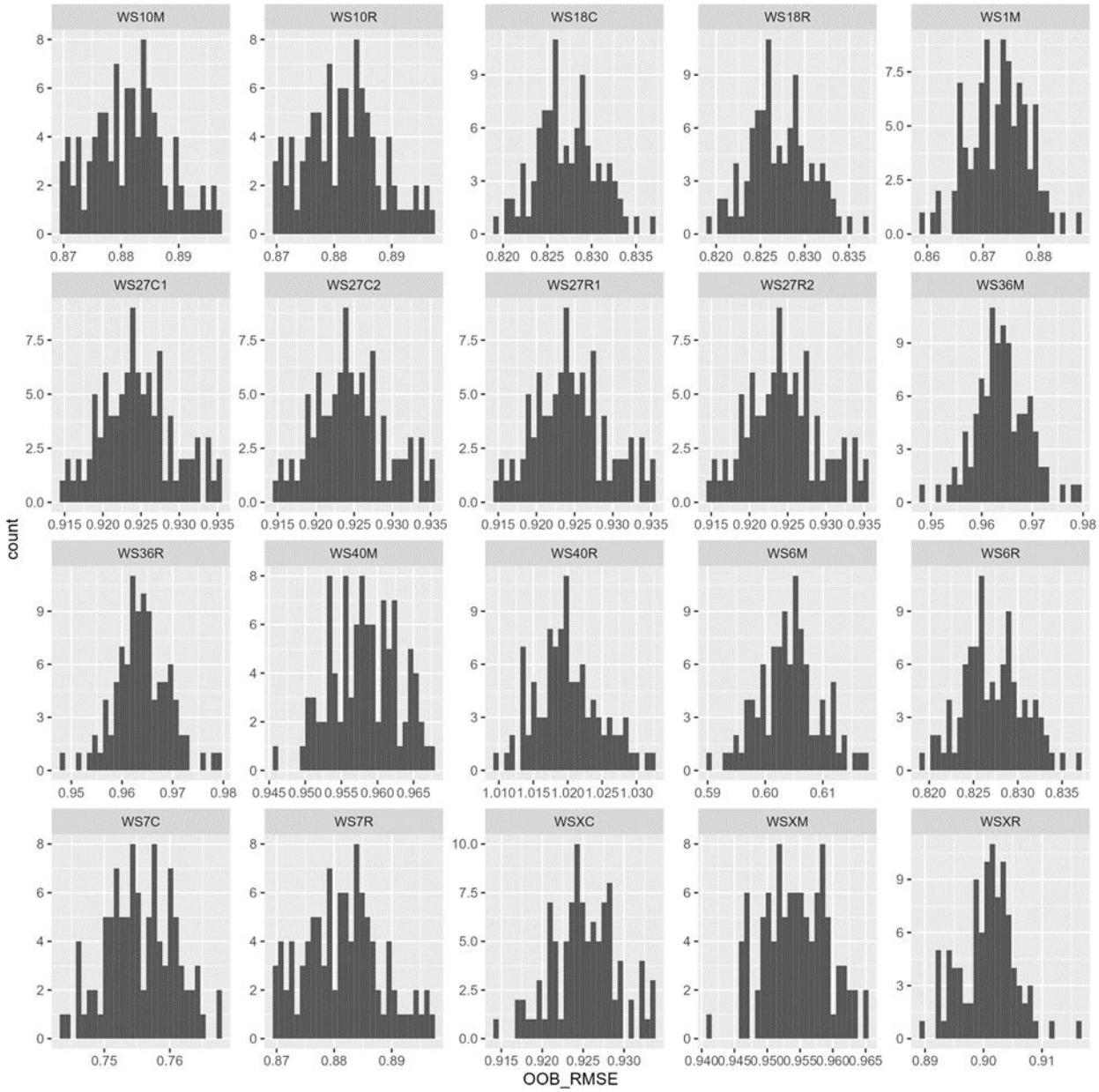

Model 2. Variable Importance

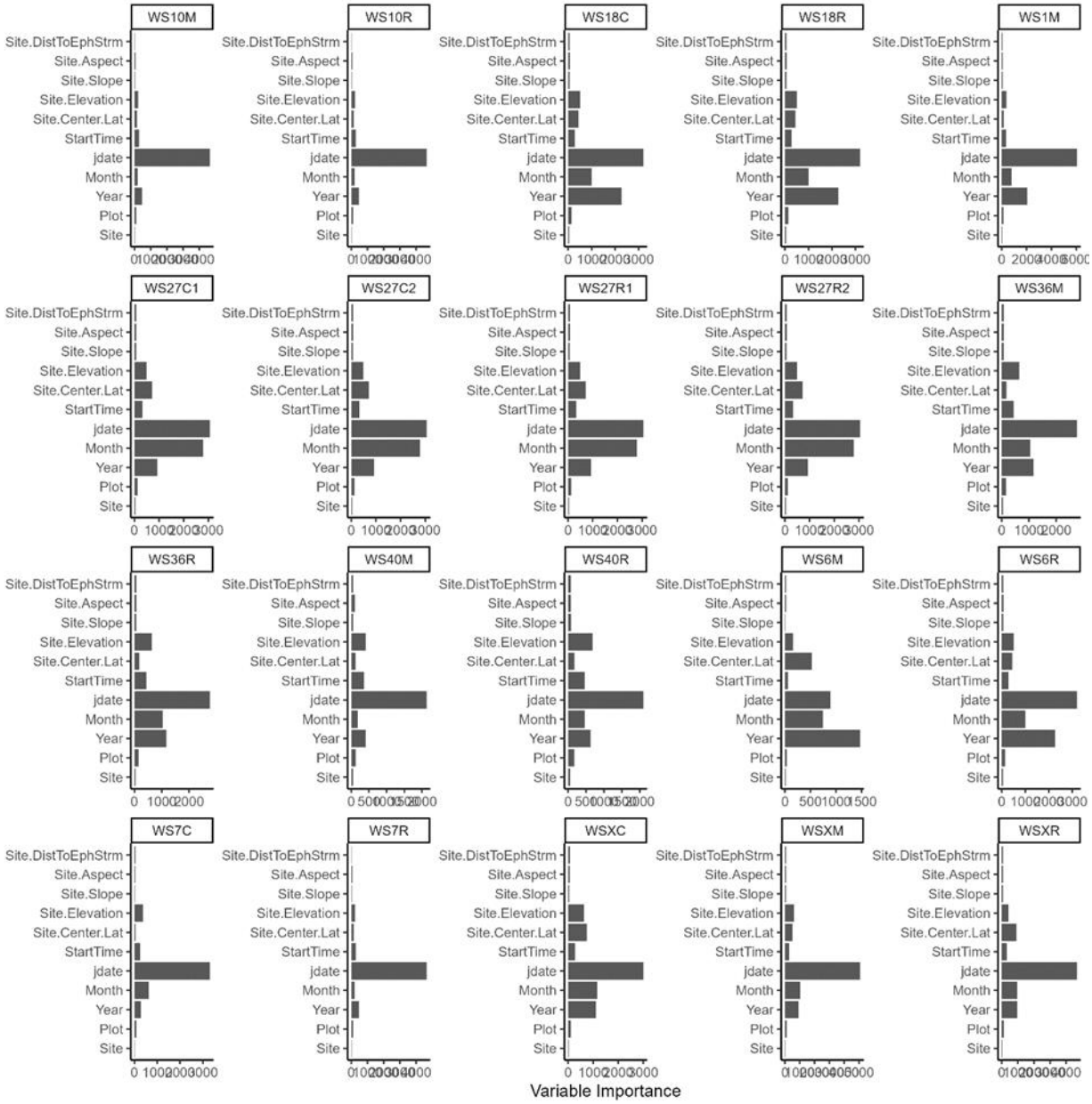

Model 3. Predicted vs. Measured

predicted (blue), measured (red)

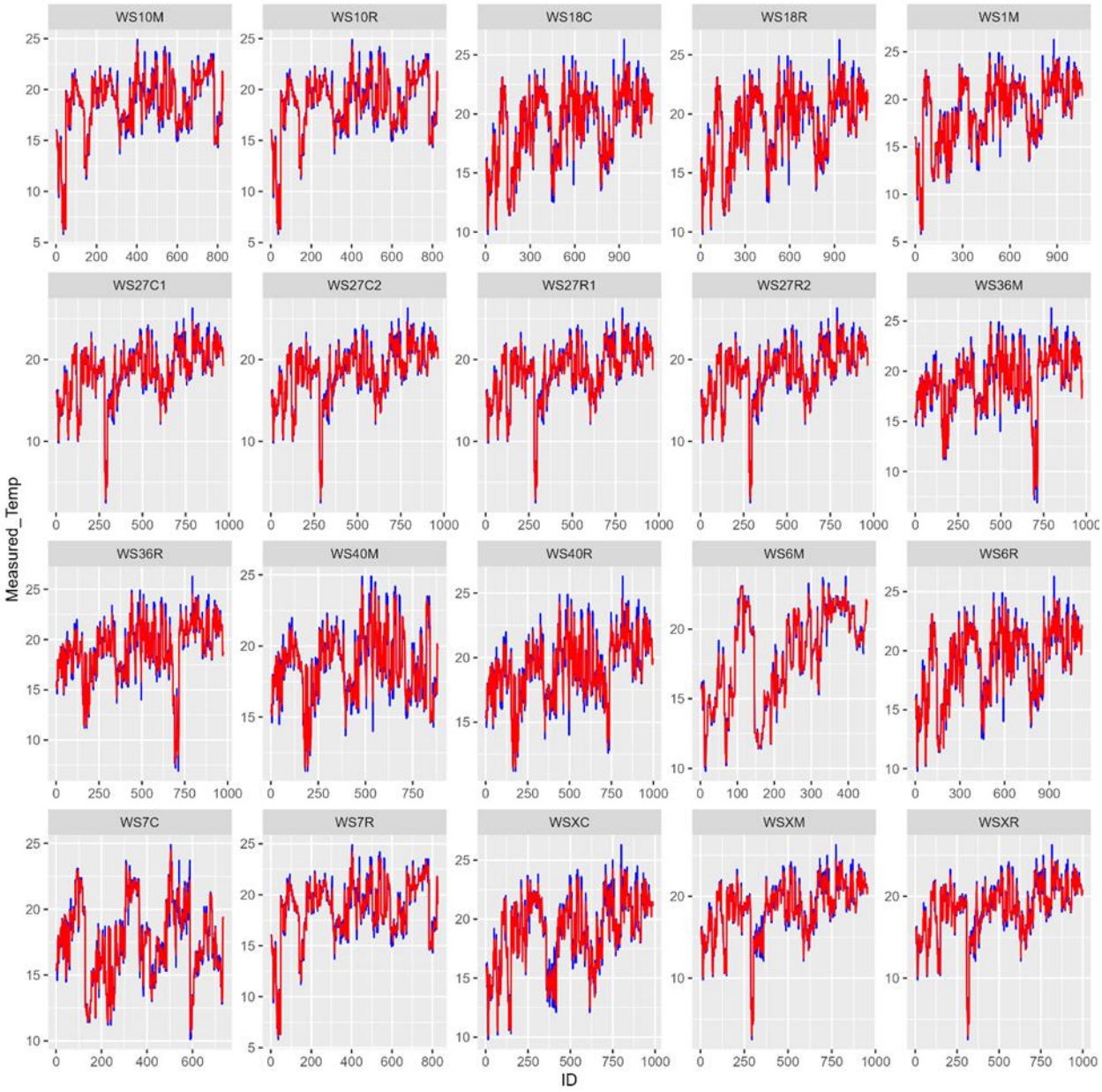

APPENDIX C

MODEL ASSESSMENTS

1 The model

1.1 Data variables

Dependent variables (predicted)

- Expected abundance (λ)
- Expected availability (ω)
- Expected probability of conditional capture (ρ)

Independent variables (predictors) on the ecological process

- Elevation ($elev$)
- Distance to the nearest ephemeral stream ($dist$)
- Northness ($north$)

Independent variables (predictors) on the observation processes

- Vapor pressure deficit (vpd)
- Cumulative precipitation ($precip$)
- Ground vegetation cover (veg)

1.2 Likelihood function and parameters

We used an integrated hierarchical modeling approach in a Bayesian framework to generate estimates of salamander abundance with data from both designs. We selected geomorphic and weather-related model covariates that represented important correlates

of soil hydrology and hydroclimate in southern Appalachia. We included elevation, stream distance, and aspect as predictors of abundance, and we included vapor pressure deficit and precipitation as predictors of salamander availability. The parameters we placed on abundance reflect temporally stable proxies of soil moisture, precipitation, and humidity that we expected to affect salamander abundance, and the parameters we place on availability reflect orographic patterns in precipitation and temperature that shape weather and are expected to affect salamander surface activity (Gade et al. 2020). We chose to include ephemeral, seasonal, and perennial streams in our definition of stream because of their role in hillslope hydrology and stream-breeding salamander life history. We used vegetation coverage as a predictor of salamander conditional capture probability because we expected vegetation to increase habitat complexity and make it more difficult for observers to detect salamanders.

1.3 Prior distribution

We chose to use vague uninformative priors on all of our parameters.

1.4 Formal specification

We integrated multinomial and binomial mixture models to estimate the terrestrial abundance (λ), availability (ω), and conditional capture probability (ρ) of salamanders at each plot every year. We modeled the ecological process of abundance as a function of elevation ($Elev$), aspect ($Northness$), and stream distance ($Dist$) with an interaction between elevation and stream distance. We specified that the abundance intercept varied among plots and years to allow populations to be open among years.

$$\log(\lambda_i) = \beta_0 + \beta_1 Elev_i + \beta_2 Dist_i + \beta_3 Dist_i Elev_i + \beta_4 Northness_i$$

$$N_i \sim Poisson(\lambda_i)$$

We jointly modeled availability as a function of vapor pressure deficit (*VPD*) and cumulative precipitation 5 days prior to a sampling event (*Precip*). We included a site-specific random effect on availability to account for spatial autocorrelation amongst plots within sites.

$$logit(\omega_j) = \omega_0 + \omega_1 VPD_j + \omega_j Precip_j + SiteEffect_j$$

$$\Omega_j \sim Binonial(\omega_j, N_i)$$

We jointly estimated the conditional capture probability of the first quarter or first pass of a survey (ρ) as a function of observer-estimated ground vegetation cover and a random effect of plot visit but modeled this portion of the observation process separately for each data set. The detection process for count data collected using the Robust Design transforms this estimate (ρ) into an estimate of the conditional capture probability of a survey ($1 - (1 - \rho_k)^4$) before drawing counts from a binomial process. In contrast, the detection process for count data collected using the depletion design passes this estimate (ρ) through a multinomial process which estimates the probability a surface-active

salamander is captured in the first, second, third, and fourth pass before estimating the probability that a surface-active salamander is not captured ($(1-\rho_k)^4$). From this multinomial process an estimate of the conditional capture probability of a survey ($1-(1-\rho_k)^4$) is derived and used to draw counts from a binomial process. These expected counts are then combined with the five pass-level conditional capture probabilities to draw counts from a multinomial process.

Robust Observation Process	**Depletion observation process**
$logit(\rho_k) = \alpha_0 + \alpha_1 Veg_k + VisitEffect_k$	$logit(\rho_k) = \alpha_0 + \alpha_1 Veg_k + VisitEffect_k$
$\rho.eff_k = 1-(1-\rho_k)^4$	$\pi_{k,1} = \rho_k$ $\pi_{k,2} = (1-\rho_k) \times \rho_k$ $\pi_{k,3} = (1-\rho_k)^2 \times \rho_k$ $\pi_{k,4} = (1-\rho_k)^3 \times \rho_k$ $\pi_{k,5} = (1-\rho_k)^4$
$y.r_k \sim Binomial(p.eff_k, \Omega_j)$	$n_k \sim Binomial((1-\pi_{k,5}), \Omega_j)$
	$\{(y.d_{k,1:4}\} \sim Multinomial(n_k, (\pi_{k,1:4}/(1-\pi_{k,5})))$

1.5 Prior predictive check

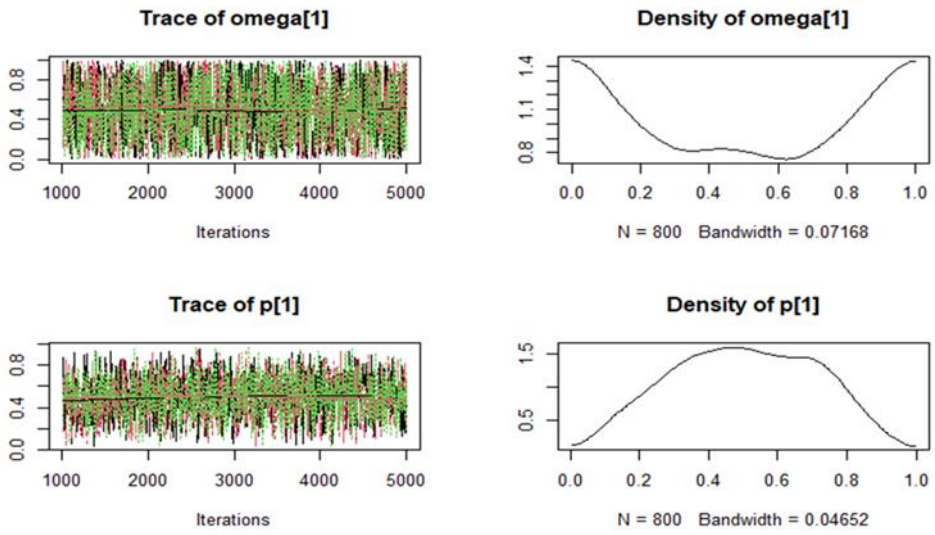

1.6 Model assumptions

The model of detection under the depletion design assumes that we are able to sufficiently deplete the true population (i.e. that counts decrease with each pass). Below are average counts for each pass.

	Mountain Dusky Species	**Blue Ridge Two-lined**
Average count		
Pass-1	0.127	0.174
Pass-2	0.101	0.119
Pass-3	0.085	0.100
Pass-4	0.083	0.081

2 Computation

2.1 MCMC chain convergence ($\hat{R}$)

	Mountain Dusky Species	**Blue Ridge Two-lined**
beta 1	1.136	1.012
beta 2	1.021	1.022
beta 3	1.148	1.032
beta 4	1.015	1.003
omega 1	1.015	1.011
omega 2	1.019	1.005
alpha 1	1.027	1.052

2.1.1 Mountain Dusky Trace plots

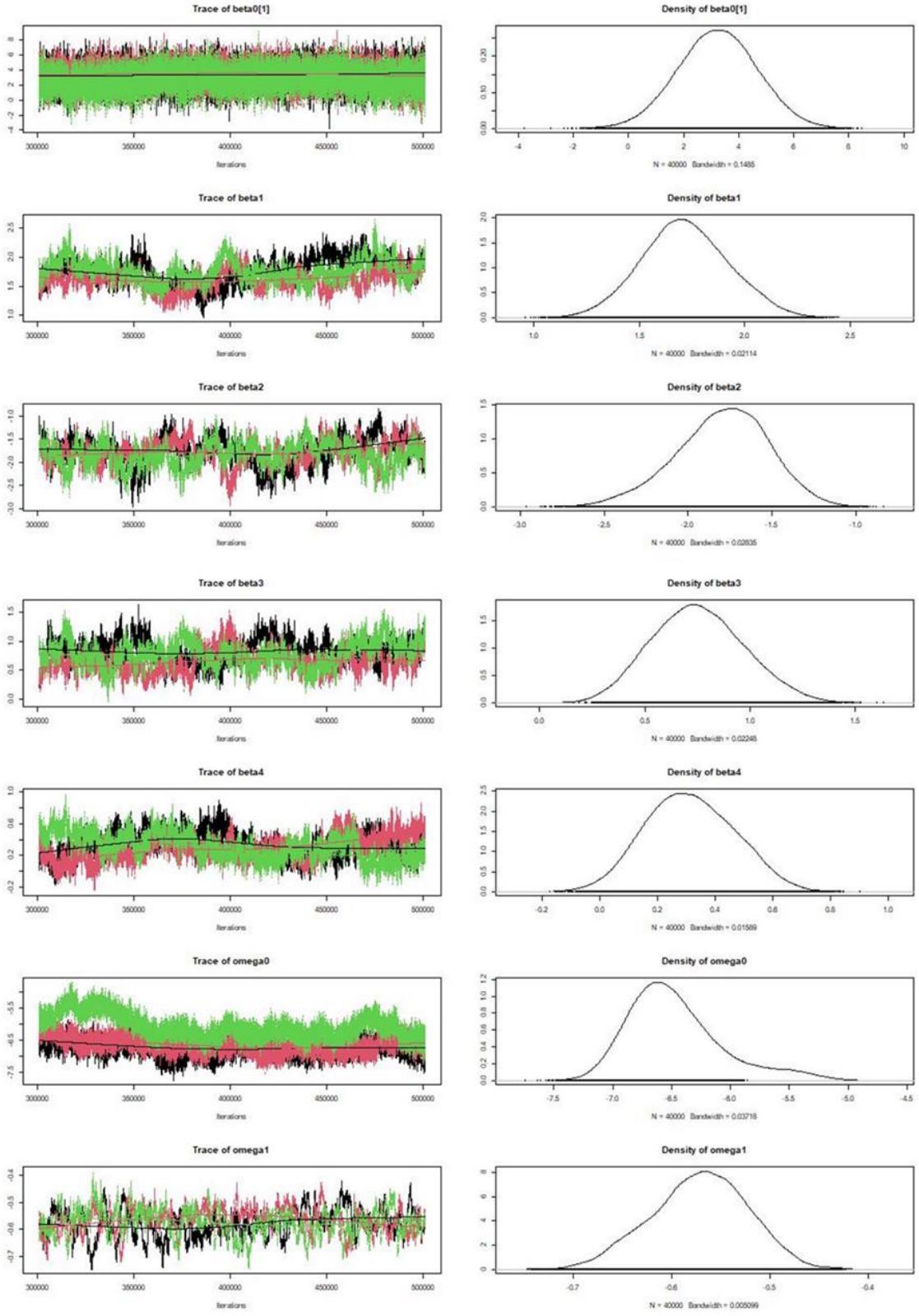

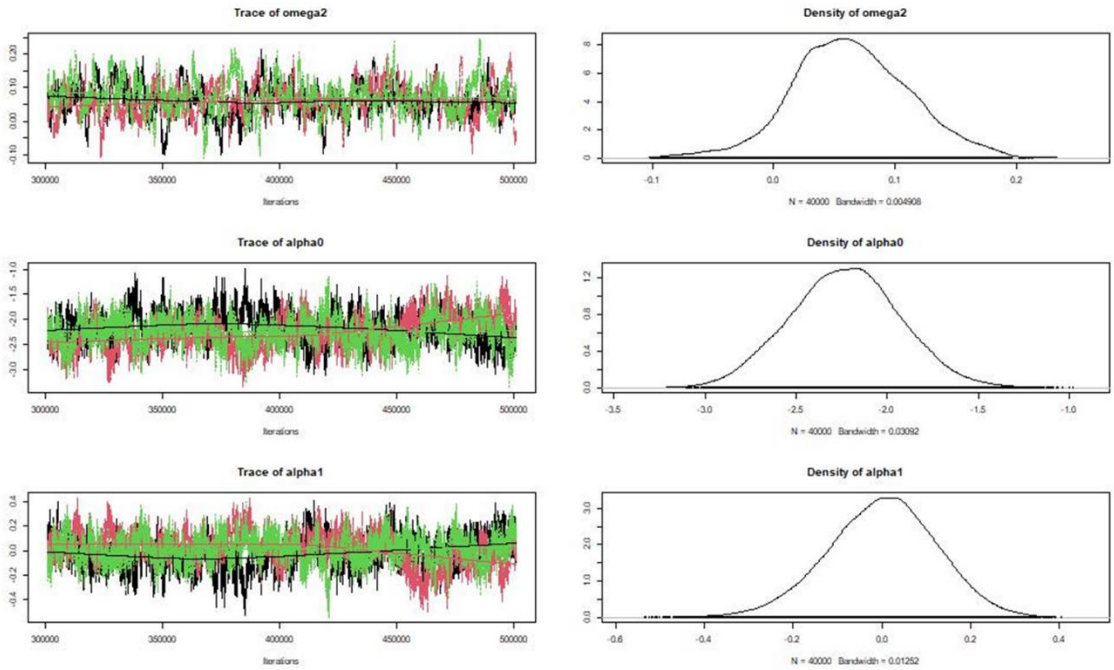

2.1.2 Blue Ridge Two-Lined Trace plots

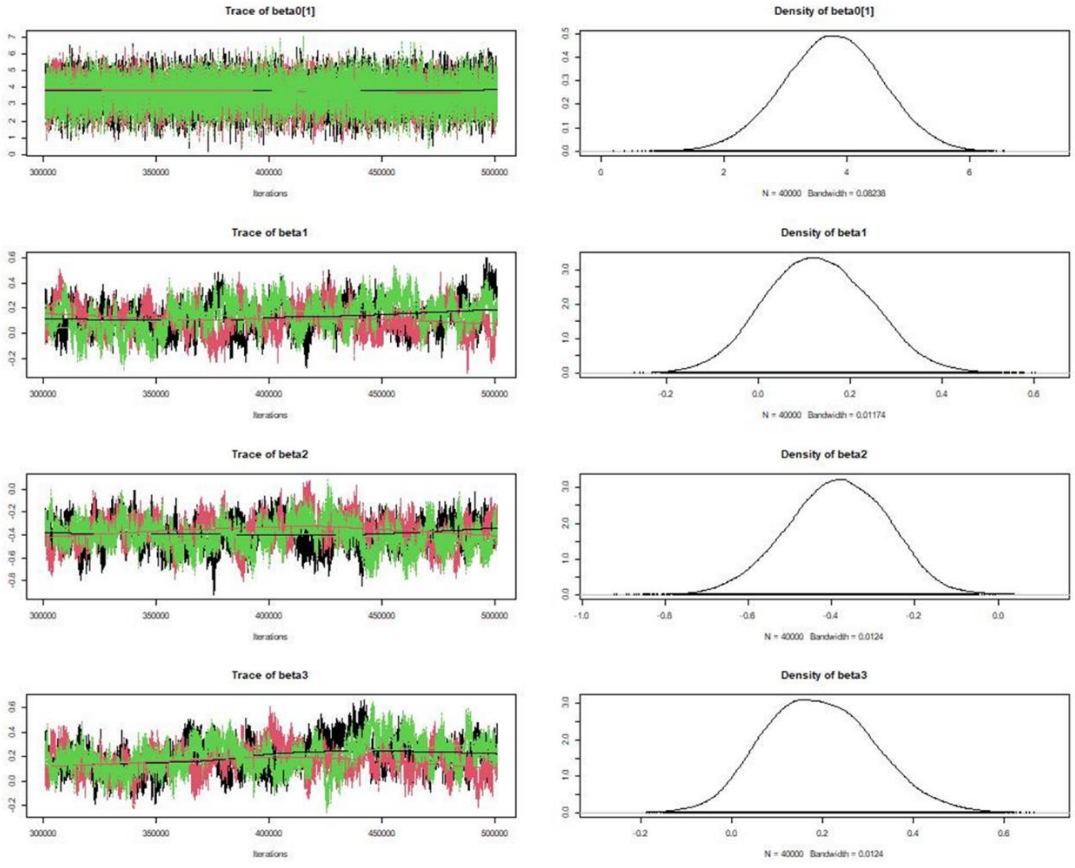

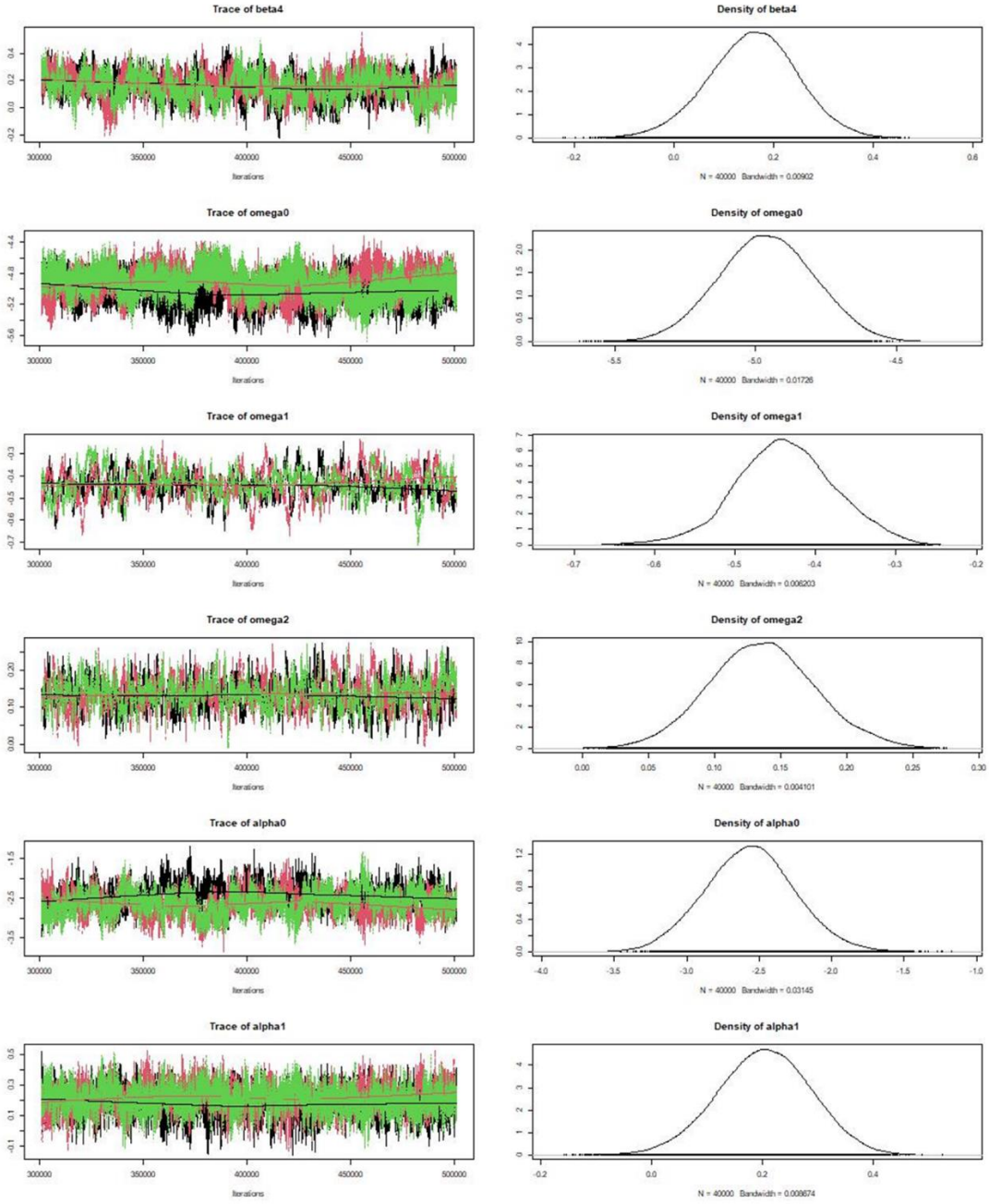
Trace of beta4
Density of beta4
Trace of omega0
Density of omega0
Trace of omega1
Density of omega1
Trace of omega2
Density of omega2
Trace of alpha0
Density of alpha0
Trace of alpha1
Density of alpha1
Iterations
N = 40000 Bandwidth = 0.00902
N = 40000 Bandwidth = 0.01726
N = 40000 Bandwidth = 0.006203
N = 40000 Bandwidth = 0.004101
N = 40000 Bandwidth = 0.03145
N = 40000 Bandwidth = 0.008674

2.2 MCMC chain resolution (i.e. effective sample size)

	Mountain Dusky Species	**Blue Ridge Two-lined**
lambda	9 - 4850	65 - 120000
beta0	8 - 302	111 - 120000
beta1	19	174
beta2	129	96
beta3	18	71
beta4	173	626
omega	1 - 138	20 - 19988
omega0	5	20
omega1	158	347
omega2	113	442
p	166 - 120000	323 - 120000
alpha0	102	19
alpha	91	43

3 Posterior distributions

3.1 Posterior predictive check

We assessed model fit using Bayesian p-values and scatterplots of associated discrepancy measures (Gelman et al. 2021.; Schaub and Kéry 2022) as well as chi-squared p-values. We used mean absolute error to measure the discrepancy between observed and expected survey level counts (drawn from binomial distributions), and we used the median chi-squared p-value to measure the discrepancy between observed and expected pass level counts (drawn from a multinomial distribution). The discrepancy values we used to calculate our Bayesian p-values allowed us to assess how well our model's error structure

approximates or "fits" the error structure of our data. Bayesian p-values close to 0.5 indicate an appropriate error structure, whereas values more extreme than .05 or .95 can be indicative of poor fit. The median chi-squared p-value we used to assess our model's fit to pass-level counts allowed us to assess how likely our expected counts (samples drawn from all three MCMC chain) are to match the counts we observed. A chi-squared p-value greater than 0.05 indicates that we cannot reject the null, which states that our expected counts match our observed counts.

Bayesian p-values and chi-squared p-values for the Robust and Depletion observation processes fit to Mountain Dusky and Blue Ridge Two-Lined counts.

	Mountain Dusky Species	**Blue Ridge Two-Lined**
Robust observation process		
Survey counts $(y.r_k)$	0.541	0.519
Depletion observation process		
Survey counts (n_k)	0.595	0.667
Pass counts $(y.d_{k,1-4})$	0.428	0.417
Pass counts range	0.018-0.951	0.015-0.927
Percent poorly fit pass counts	0.022	0.027

Scatter plots of discrepancy measures

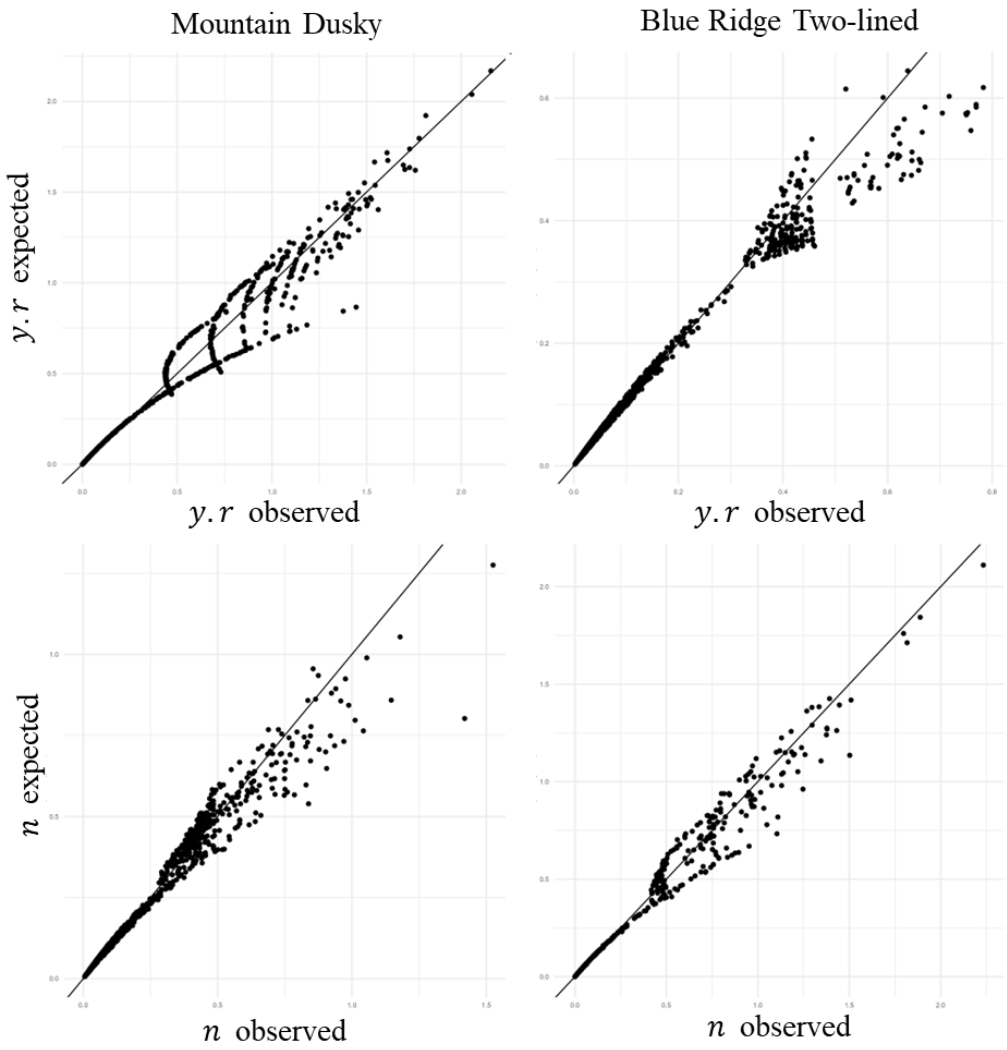

3.2 Summary of posteriors

Parameter estimates and Bayesian credible intervals from integrated abundance, availability, and detection (e.g. conditional capture probability) models for the two focal taxa. Estimates of abundance, availability, and detection are on the log and logit scale.

	Mountain Dusky Species			**Blue Ridge Two-Lined**		
	Mean	**2.5%**	**97.5**	**Mean**	**2.5%**	**97.5**
Abundance	12.527	0.004	95.983	3.158	0.312	12.273
Intercept	3.226	0.407	5.989	3.893	2.238	5.512
Elevation	1.719	1.322	2.133	0.131	-0.088	0.359
Distance	-1.797	-2.389	-1.290	-0.385	-0.629	-0.158
Elevation × Distance	0.754	0.373	1.201	0.193	-0.012	0.442
Northness	0.313	0.043	0.617	0.158	-0.008	0.330
Availability	0.006	0.000	0.059	0.008	0.001	0.034
Intercept	-6.468	-7.068	-5.433	-4.961	-5.267	-4.634
VPD	-0.572	-0.665	-0.479	-0.438	-0.553	-0.314
Precipitation	0.064	-0.023	0.163	0.136	0.064	0.218
Detection	0.134	0.016	0.462	0.157	0.009	0.615
Intercept	-2.232	-2.778	-1.632	-2.563	-3.121	-1.943
Vegetation	0.000	-0.233	0.234	0.203	0.046	0.366

3.2.1 Mountain Dusky posterior distribution plots

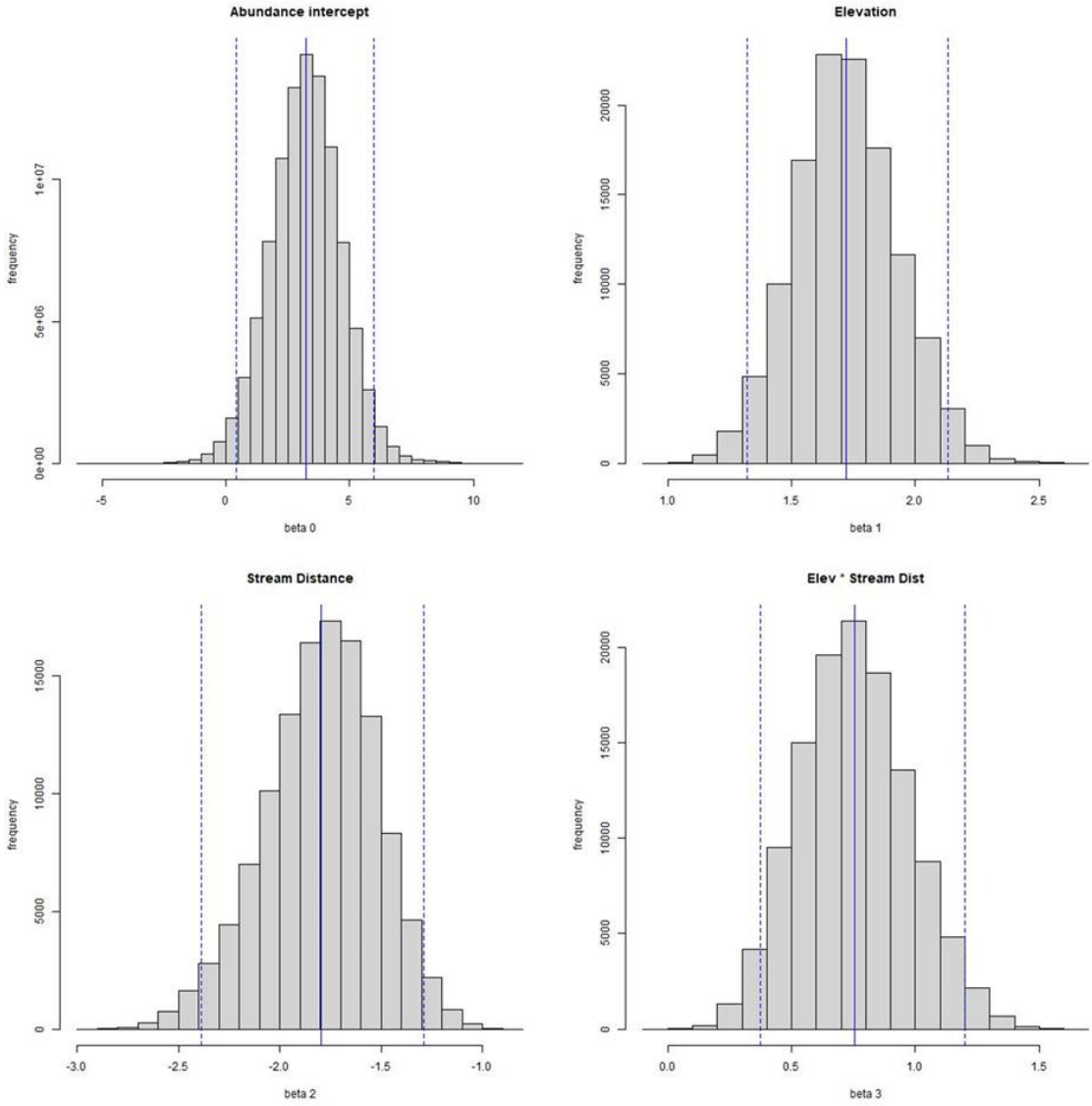

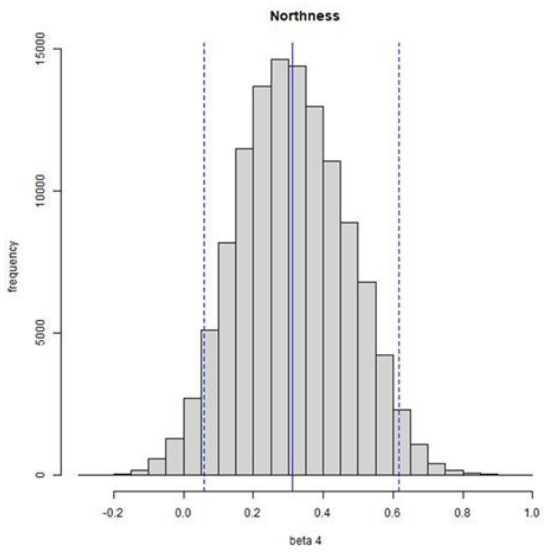
Northness
frequency
0
5000
10000
15000
-0.2
0.0
0.2
0.4
0.6
0.8
1.0
beta 4

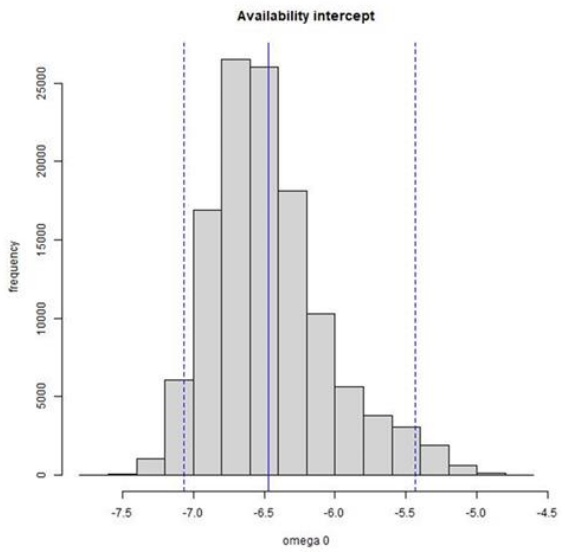
Availability intercept
frequency
0
5000
10000
15000
20000
25000
-7.5
-7.0
-6.5
-6.0
-5.5
-5.0
-4.5
omega 0

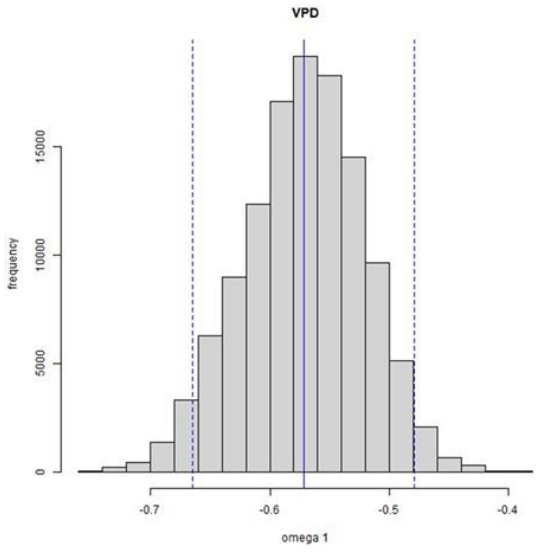
VPD
frequency
0
5000
10000
15000
-0.7
-0.6
-0.5
-0.4
omega 1

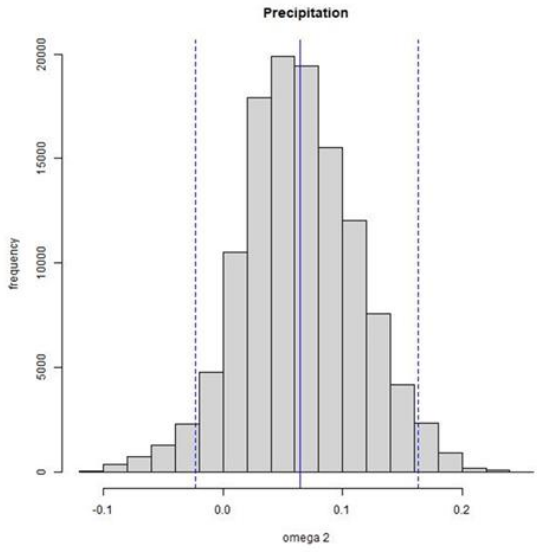
Precipitation
frequency
0
5000
10000
15000
20000
-0.1
0.0
0.1
0.2
omega 2

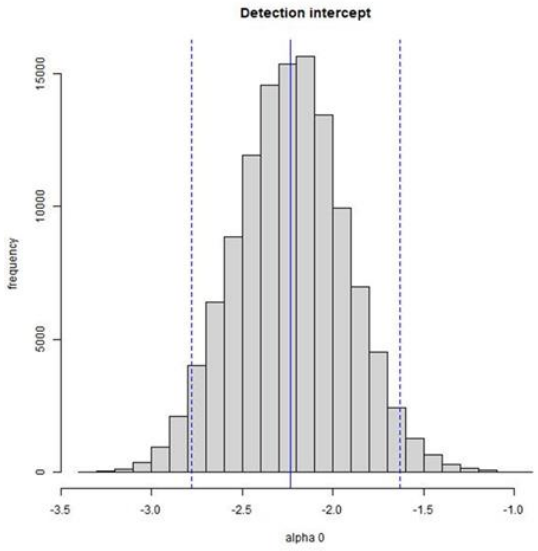
Detection intercept
frequency
0
5000
10000
15000
-3.5
-3.0
-2.5
-2.0
-1.5
-1.0
alpha 0

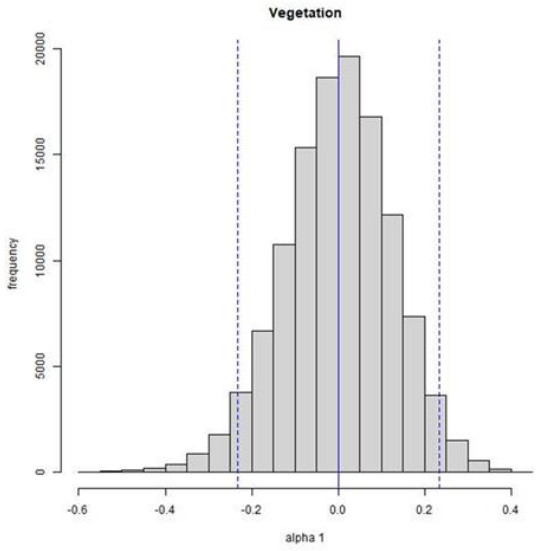
Vegetation
frequency
0
5000
10000
15000
20000
-0.6
-0.4
-0.2
0.0
0.2
0.4
alpha 1

3.2.2 Blue Ridge Two-lined Posterior distribution plots

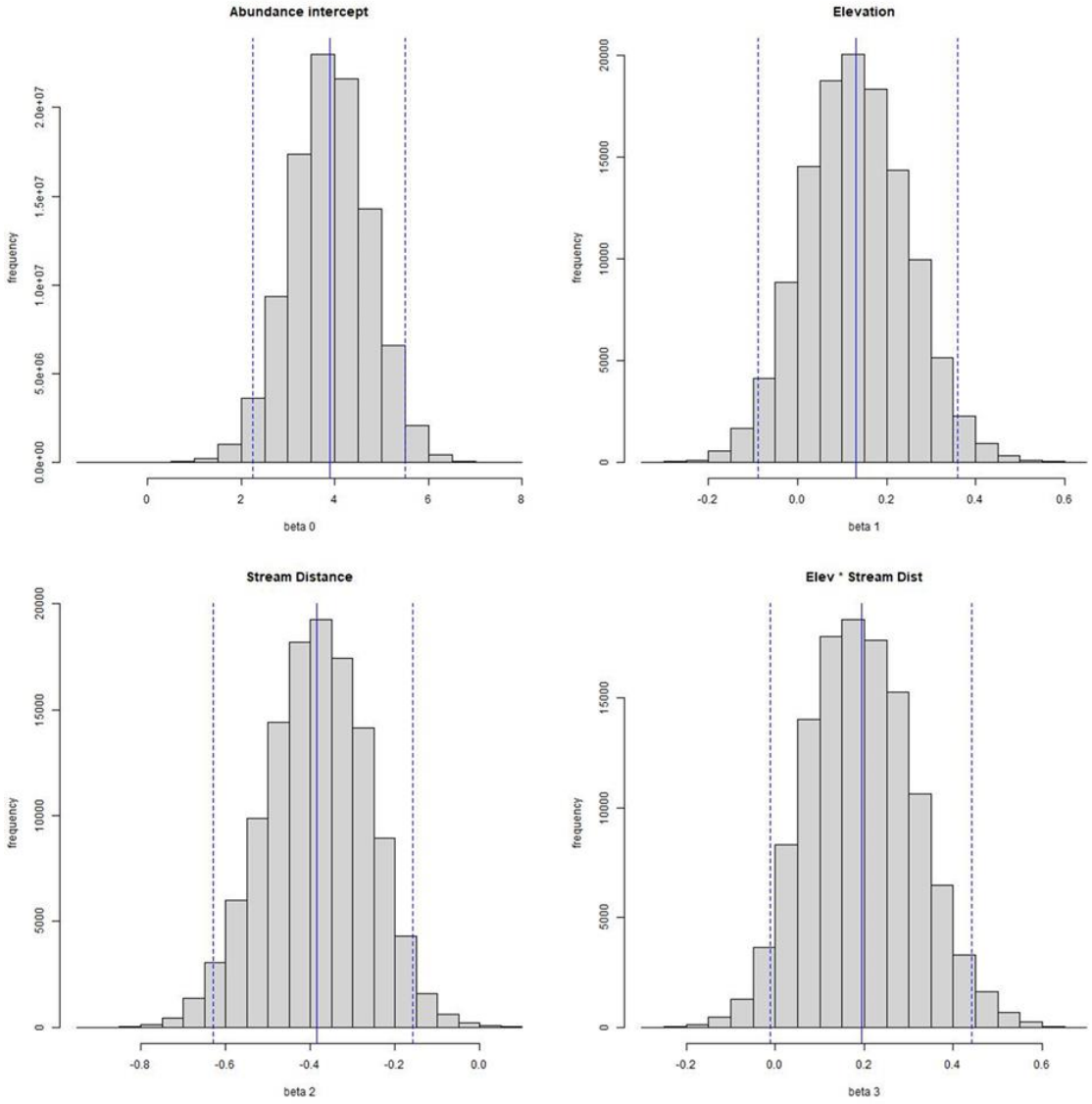

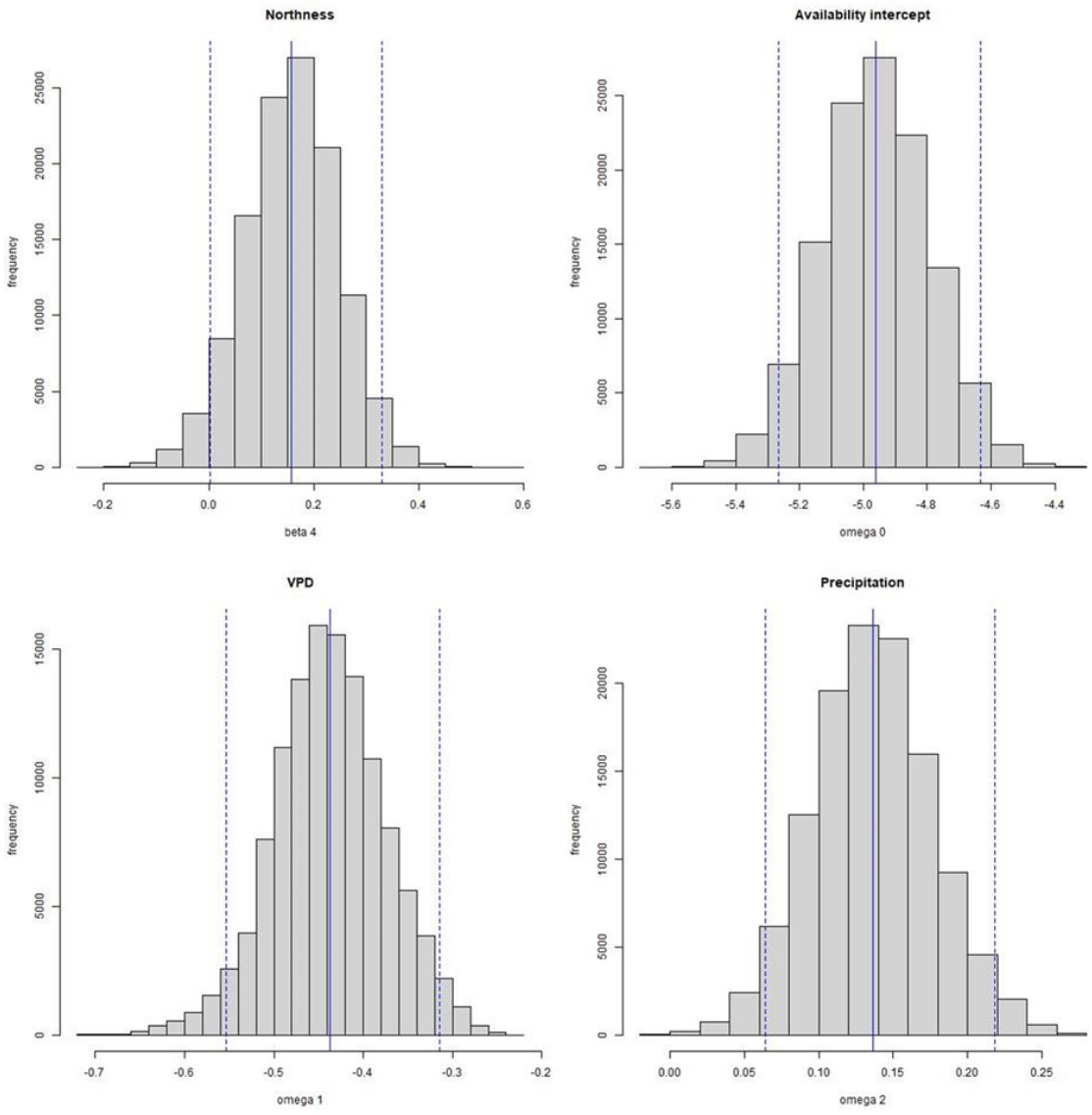
Northness
frequency
beta 4
Availability intercept
frequency
omega 0
VPD
frequency
omega 1
Precipitation
frequency
omega 2

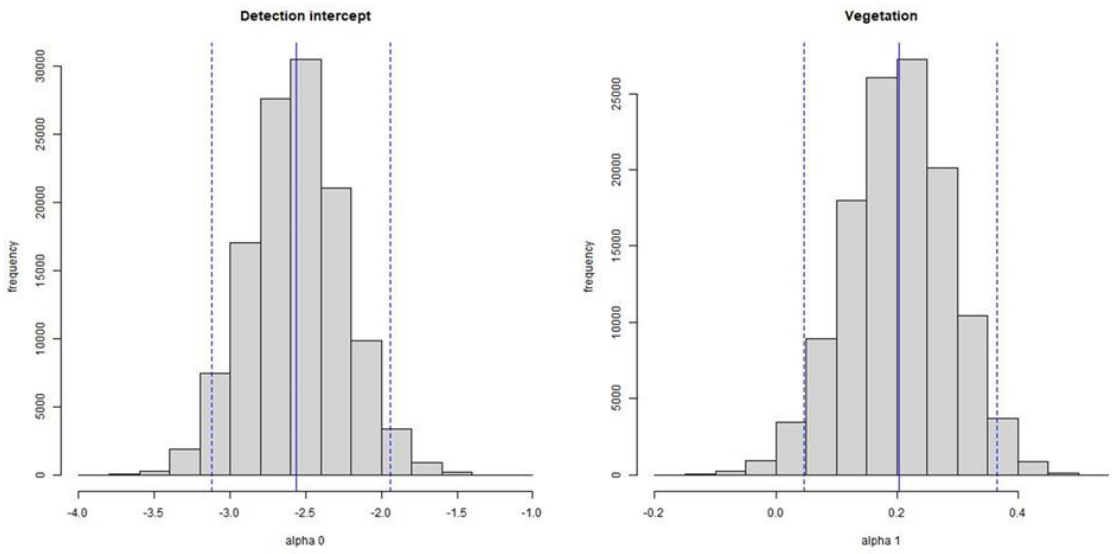

4 Sensitivity analysis

4.1 Prior sensitivity

We chose to use vague uninformative priors (dnorm(0,1)) for our final analysis. Post-hoc iterations of the model fit with more narrow but equally uninformative priors (dnorm(0,0.33)) produced similar results. This and our prior predictive check give us confidence that our results are not sensitive to the priors we chose.

5 Predictive accuracy

To validate the model's predictive accuracy and estimate prediction error, we withheld data collected in 2023 at three sites in watershed 32 at Coweeta Hydrological Laboratory and used the fitted model to predict counts observed at the sites in 2023. The three sites selected are the only sites in our integrated dataset that were sampled every year from 2016 to 2023. They are located centrally within the elevational and latitudinal range of

our data but share a southeastern aspect. Collectively they represent a relatively average area with high temporal replication.

	Mountain Dusky Species	**Blue Ridge Two-lined**
Pass-1	0.019	0.088
Pass-2	0.015	0.072
Pass-3	0.012	0.064
Pass-4	0.010	0.081